

12-27-1962

The Leakage Neutron Spectrum of a Spherical Critical Assembly of U233

Larry E. Bobisud

Follow this and additional works at: https://digitalrepository.unm.edu/phyc_etds



Part of the [Astrophysics and Astronomy Commons](#), and the [Physics Commons](#)

Recommended Citation

Bobisud, Larry E.. "The Leakage Neutron Spectrum of a Spherical Critical Assembly of U233." (1962).
https://digitalrepository.unm.edu/phyc_etds/93

This Thesis is brought to you for free and open access by the Electronic Theses and Dissertations at UNM Digital Repository. It has been accepted for inclusion in Physics & Astronomy ETDs by an authorized administrator of UNM Digital Repository. For more information, please contact disc@unm.edu.

UNIVERSITY OF NEW MEXICO-GENERAL LIBRARY



A14425 250958

378.789

Un30bo

1963

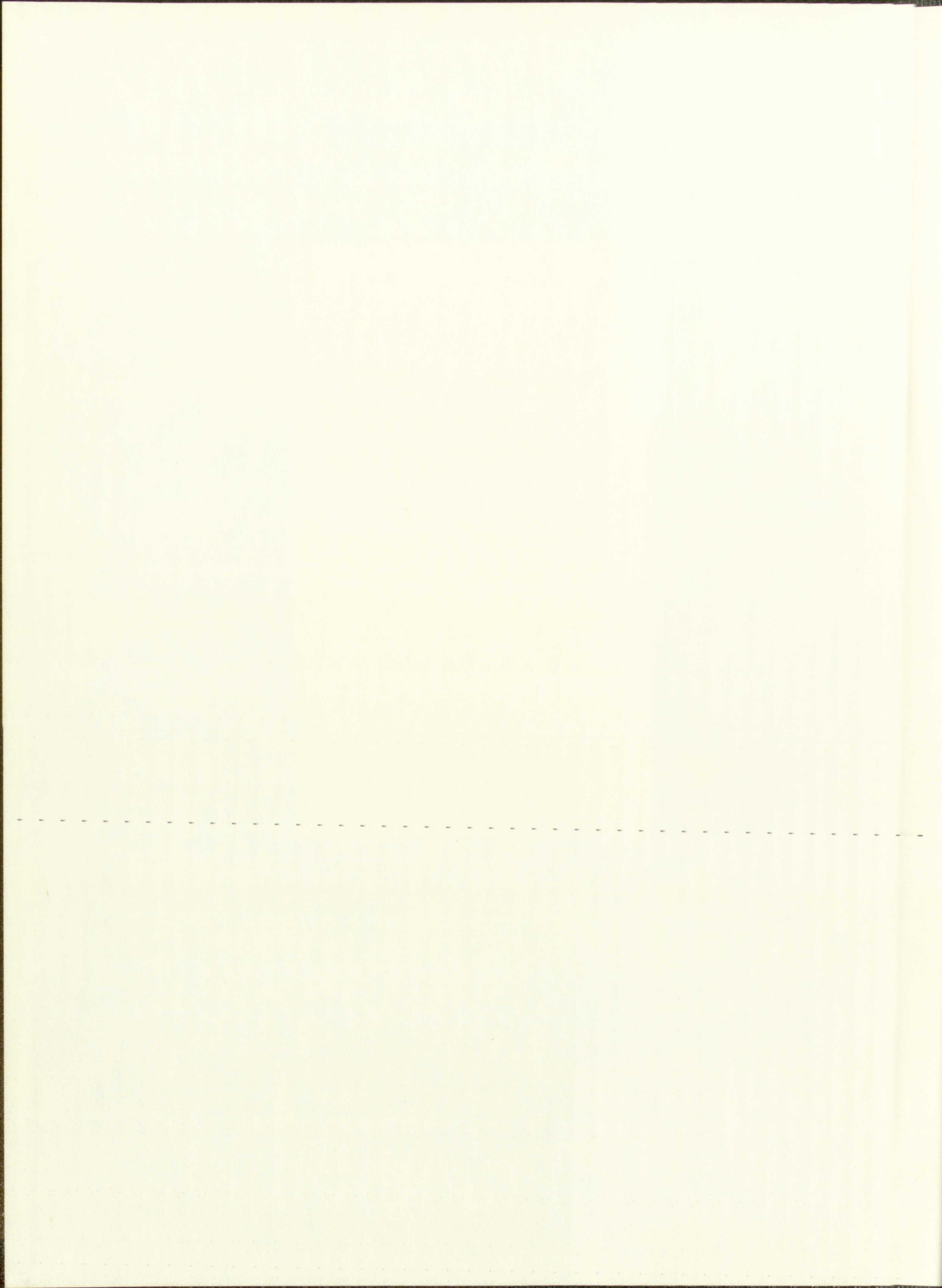
cop. 2

THE LIBRARY
UNIVERSITY OF NEW MEXICO



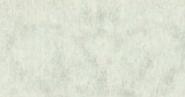
Call No.
378.789
Un30bo
1963
cop.2

Accession
Number
307821



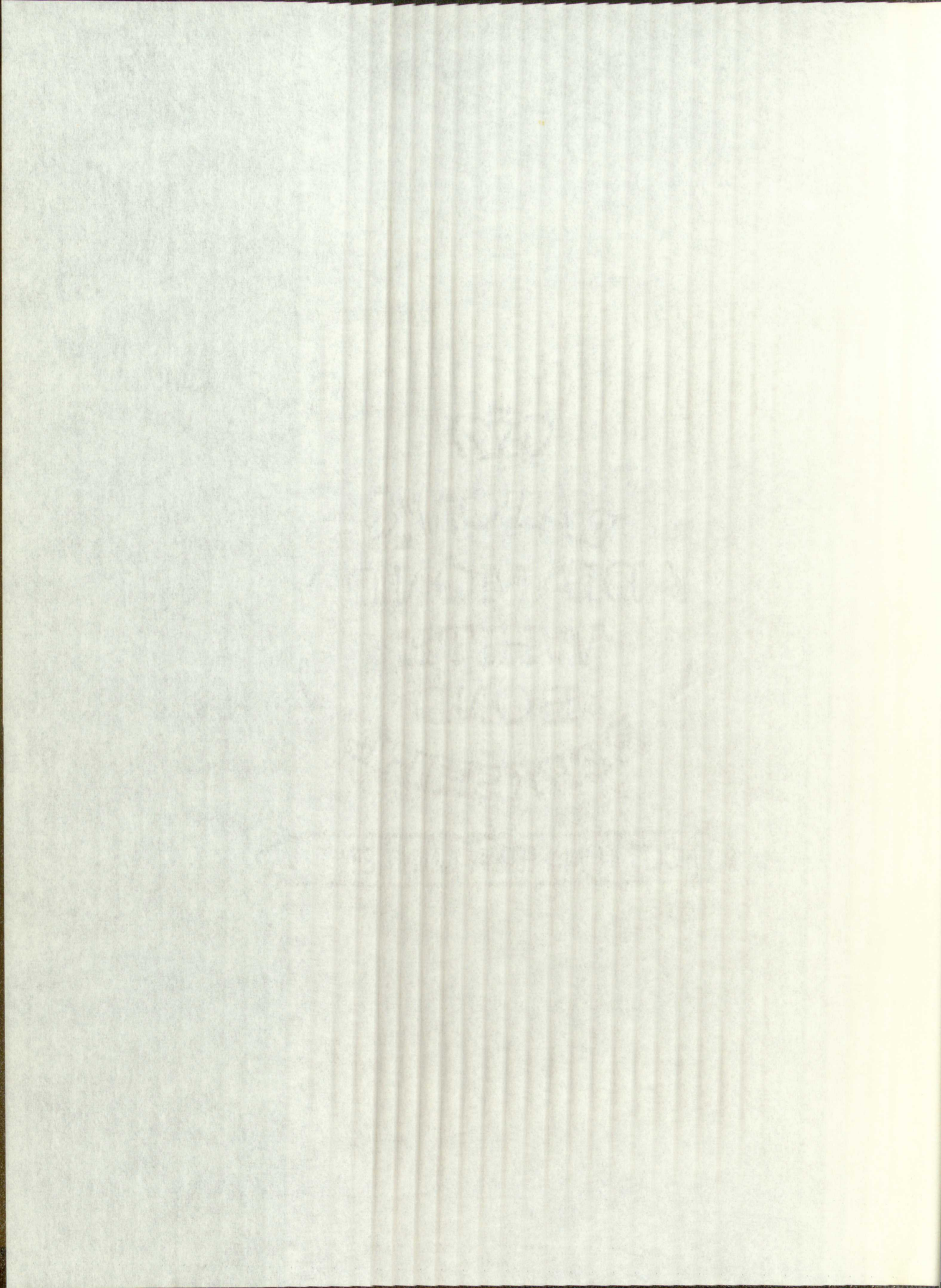






WALTON
BRITAIN
WHITE
BOARD
STRENGTH

WALTON WHITE BOARD STRENGTH



UNIVERSITY OF NEW MEXICO LIBRARY

MANUSCRIPT THESES

Unpublished theses submitted for the Master's and Doctor's degrees and deposited in the University of New Mexico Library are open for inspection, but are to be used only with due regard to the rights of the authors. Bibliographical references may be noted, but passages may be copied only with the permission of the authors, and proper credit must be given in subsequent written or published work. Extensive copying or publication of the thesis in whole or in part requires also the consent of the Dean of the Graduate School of the University of New Mexico.

This thesis by Larry E. Bobisud
has been used by the following persons, whose signatures attest their acceptance of the above restrictions.

A Library which borrows this thesis for use by its patrons is expected to secure the signature of each user.

NAME AND ADDRESS

DATE

MANUSCRIPT THESIS

Unpublished thesis submitted for the Master's and Doctor's degrees and deposited in the University of New Mexico Library are open for inspection, but are to be used only with due regard to the rights of the author. Bibliographical references may be noted, but passages may be copied only with the permission of the author, and proper credit must be given in subsequent written or published work. Extensive copying or publication of the thesis in whole or in part requires also the consent of the Dean of the Graduate School of the University of New Mexico.

This thesis by Jerry E. Johnson has been used by the following persons, whose signatures attest their acceptance of the above restrictions.

A library which borrows this thesis for use by its patrons is expected to secure the signature of each user.

NAME AND ADDRESS _____
DATE _____

THE LEAKAGE NEUTRON SPECTRUM
OF A SPHERICAL CRITICAL ASSEMBLY OF U²³³

By

Larry E. Bobisud

A Thesis

Submitted in Partial Fulfillment of the
Requirements for the Degree of
Master of Science in Physics

The University of New Mexico

1962

THE LIBRARY OF THE UNIVERSITY OF TORONTO
BY A SPECIAL DIVISION APPROVED BY THE



BY
JERRY A. HARRIS

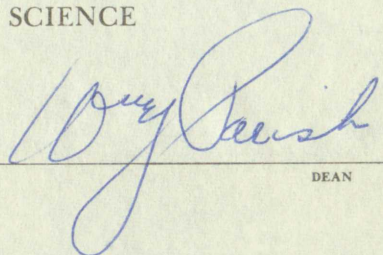
A Thesis
Submitted in Partial Fulfillment of the
Requirements for the Degree of
Master of Science in Physics

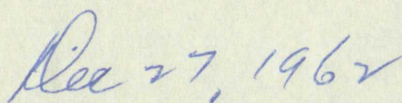
The University of New Mexico

1962

This thesis, directed and approved by the candidate's committee, has been accepted by the Graduate Committee of the University of New Mexico in partial fulfillment of the requirements for the degree of

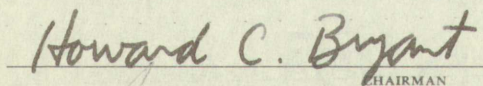
MASTER OF SCIENCE

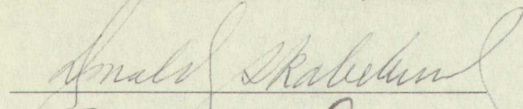

DEAN

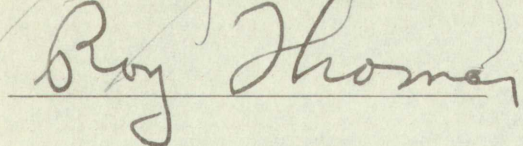


DATE

Thesis committee


CHAIRMAN





This thesis directed and approved by the candidate's com-
mittee, has been accepted by the Graduate Committee of the
University of New Mexico in partial fulfillment of the require-
ments for the degree of

MASTER OF SCIENCE

[Signature]
NAME

Dec. 27, 1964
DATE

Thesis committee

Howard C. Bryant
MEMBER

[Signature]
MEMBER

Ray Johnson
MEMBER

378.789
un 30 no
1963
Cop. 2

TABLE OF CONTENTS

| | Page |
|---|------|
| I. INTRODUCTION | 1 |
| II. EXPERIMENTAL ARRANGEMENT AND ANALYSIS | 2 |
| III. EXPERIMENTAL RESULTS | 15 |
| IV. APPLICATION OF THE NEUTRON TRANSPORT EQUATION TO SPHERICAL CRITICAL ASSEMBLIES | 23 |
| APPENDICES | 35 |

307821

378.878
2008-2009
1968
2-20-09

TABLE OF CONTENTS

| Page | |
|------|--|
| 1 | I. INTRODUCTION |
| 2 | II. EXPERIMENTAL ARRANGEMENT AND THEORY |
| 17 | III. EXPERIMENTAL RESULTS |
| 23 | IV. APPLICATION OF THE METHOD PROPOSED IN CONNECTION TO SPHERICAL CRITICAL ANGLES |
| 37 | APPENDICES |

307821

I. INTRODUCTION

In this paper the spectrum of the neutrons escaping from a critical sphere of U^{233} is investigated experimentally and theoretically. The experimental investigation involved exposing a nuclear emulsion to the neutron flux and, after development, examining the details of the proton-recoil tracks visible in the emulsion. From the information thus derived the initial energies of the colliding neutrons were determined; combined with a correction for protons leaving the emulsion, the cross section for neutron-proton scattering, the number of protons per cubic centimeter of emulsion, and the solid angle considered, the number of neutrons per energy interval yields the energy spectrum of the incoming neutrons. The spectrum so obtained is briefly compared with the similarly obtained spectra of spherical critical assemblies of U^{235} and Pu^{239} .

For the theoretical determination of the leakage neutron spectrum, the neutron transport equation is derived under suitable assumptions. Obtained by numerical integration, the solution of this equation is presented in the form of the relative neutron flux in each of several energy intervals. Finally, the theoretical spectra of the three critical assemblies mentioned above are compared with those observed.

1. Introduction

In this paper we report on the results of our investigation into the structure and properties of the system under study. The system is characterized by its unique properties and its behavior under various conditions. The results of our experiments are presented in the following sections. The first section describes the experimental setup and the methods used to collect the data. The second section discusses the results of the measurements and compares them with theoretical predictions. The third section presents a detailed analysis of the data and discusses the implications of the findings. The fourth section concludes the paper and suggests directions for future research.

For the present, we have only a few preliminary results. The data obtained so far are consistent with the theoretical model proposed in the literature. However, further experiments are needed to confirm these results and to explore the system's behavior under different conditions. We believe that the study of this system is of great importance and we hope that our work will contribute to a better understanding of its properties.

II. EXPERIMENTAL ARRANGEMENT AND ANALYSIS

To determine experimentally the leakage neutron spectrum of the bare U^{233} critical assembly in existence at Los Alamos, a number of approximately 200 μ thick Ilford K2 nuclear emulsions were exposed for several minutes to the neutron flux present at a distance of 125 centimeters from the surface of the critical assembly. The plates were stacked two together, emulsions facing each other but separated by a thin platinum foil to prevent the possibility that a proton from one emulsion might recoil into the other; the whole plate assembly was wrapped in black paper. The accompanying illustration shows the exposure configuration.

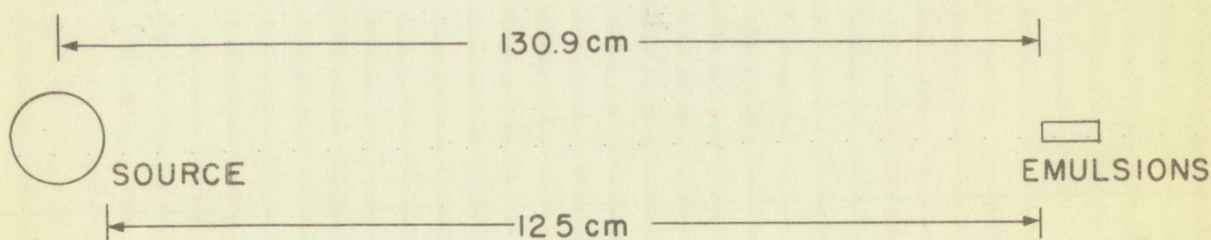


Fig. 1.--Exposure configuration

By making several exposures at differing integrated neutron flux levels (approximately 5×10^7 to 2×10^8 neutrons/cm²) at the plates, the density of tracks was optimized for ease in subsequent analysis.

A background measurement was made with the identical basic geometry to allow correction for events caused by normal background radiations (cosmic rays, etc.) and neutrons scattered into the emulsion; for the background determination, however, a polyethylene block in the form of the right frustum of a pyramid was inserted between the source and the detector in the illustrated manner. This shield was

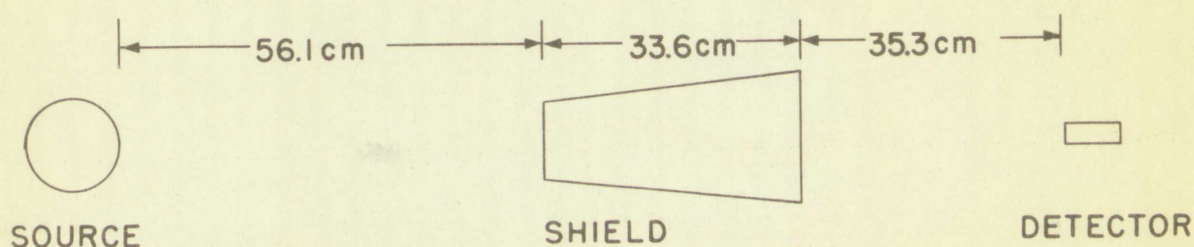


Fig. 2.--Background exposure configuration

sufficiently large (greater than three mean free paths in length) to prevent arrival at the detector of a neutron coming directly from the source.

After development¹ of the emulsions, the tracks of protons which had apparently recoiled from collisions with incident neutrons were examined using a high-power (100X) oil-immersion objective on a microscope equipped with a calibrated fine adjustment of focus and with a calibrated

¹For development techniques see J. C. Allred and A. H. Armstrong: Laboratory Handbook of Nuclear Microscopy (Los Alamos: Los Alamos Scientific Laboratory, 1951) and L. Rosen, Nuclear Emulsion Techniques for the Measurement of Neutron Energy Spectra, Nucleonics 11, No. 7, 32 (1953).

A backscattered electron image of a polymer surface, showing a granular texture. The image is inverted, with the detector in the upper left corner. The surface appears to be composed of small, irregular particles or grains.



Fig. 2.--Backscattered electron image of a polymer surface. The image shows a granular texture, characteristic of a polymer surface. The detector is located in the upper left corner of the image.

After exposure of the polymer surface to a backscattered electron beam, the surface exhibits a granular texture. This texture is characteristic of a polymer surface. The detector is located in the upper left corner of the image.

The backscattered electron image shows a granular texture, characteristic of a polymer surface. The detector is located in the upper left corner of the image.

mechanical stage. Since the index of refraction of the cedar oil is very nearly equal to that of the emulsion, use of an immersion objective obviates correction for the difference between the index of refraction of air and that of the emulsion. In addition to the projected range R_p of the track, the dimensions A and B and the angle θ , as illustrated, were determined. The angle θ was read from

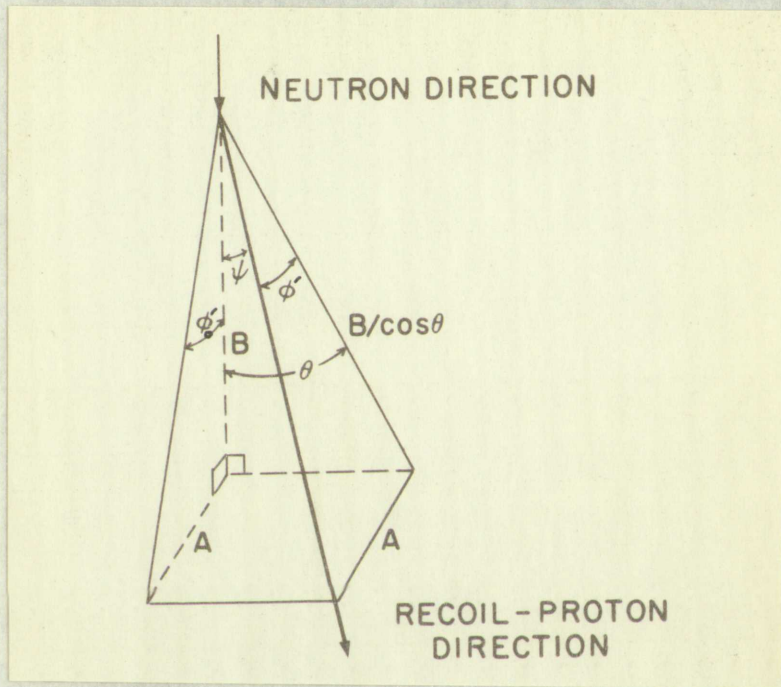


Fig. 3.--Illustration of measured quantities

a scale attached to the microscope eyepiece, which was rotated until a reference line inscribed on the reticule contained in the eyepiece coincided with the initial direction of the track. Both B and R_p are the projections of the track along a line parallel to the surface of the emulsion and parallel to the edge of the plate (and hence parallel to the direction of the incident particles). R_p is the



Fig. 8. -- Illustration of a certain condition

thus-projected range of the particle; B is some convenient portion of the track length. In general, B was taken equal to R_p for short tracks ($\leq 80 \mu$, the width of the eyepiece reticule used) and was less than R_p for long tracks.

R_p for short tracks was measured in terms of subdivisions of the eyepiece reticule (8μ per subdivision) and for long tracks (over 80μ) with the stage micrometer.

The angle ϕ' shown in Fig. 3 was not measured directly; instead, the dip distance A was measured using the calibrated fine adjustment. Since the thickness of the emulsion shrinks during development and during storage,² A is not the true dip of the proton. Let ϕ be the true dip angle; then

$$\tan \phi = \frac{KA}{B/\cos \theta'}$$

where K is the shrinkage factor, defined as

$$K = \frac{\text{True emulsion thickness before development}}{\text{Measured emulsion thickness after development}}$$

For the plates studied, which were maintained in an atmosphere of 40% relative humidity, K was of the order of 1.55, with daily variations of the order of $\pm .02$. The emulsion thickness before development was measured using a micrometer; the thickness after development was measured using the fine adjustment of the microscope. Since $\tan \phi$ thus contains the ratio of two quantities measured with the fine adjustment, any linear error in the fine adjustment cancels itself in

²The emulsion cannot shrink appreciably in its plane since it is secured to a glass backing.

This projection is...
 portion of the...
 to B for short...
 vertical...
 B, for short...
 of the...
 tracks (over...
 The angle...
 instead, the...
 fine adjustment...
 which...
 true dip of...

$$\tan \phi = \frac{KA}{B \cos \theta}$$

where K is the...
 $K =$
 For the...
 of...
 daily...
 thickness...
 the...
 adjustment...
 the ratio...
 any...
 The...
 since it is...

the calculation of ϕ . In order to avoid complications arising from curvature of field, the depths of the two ends of a track were measured with the track placed symmetrically in the field. An alternative procedure, also used, consisted of placing each end of the track in succession at the same place in the field and there determining the depth of the end grain. In both cases the dip is given, obviously, by the difference in the two depth readings.

Only tracks lying within a pyramidal solid angle defined by the (essentially arbitrary) half angles $\theta \leq 16^\circ$, $\phi \leq 16^\circ$ were used in the calculations. Only tracks running within the pyramid in the direction of the incident beam were counted; the direction of a track could in most cases be inferred from the grain density along the track since a proton ionizes more heavily near the end than at the beginning of its track.

The raw data, as described above, were processed on an IBM 704 computer, which automatically calculated the true range

$$R = R_p \sec \theta \sec \phi = R_p \sec \psi,$$

where ψ is the polar angle, for each proton whose track was measured. If a track had a sharp bend where the proton underwent a large-angle scattering from a collision with a massive nucleus, the range was measured in two (or more) portions and the computer added these partial ranges to obtain the total range. From a built-in table³ of range

³The table used is that of J. J. Wilkins, Range-Energy

The calculation of ρ is made in units of 10^{21} g/cm³ existing from symmetry of field, the number of the ions of a fixed value scattered with the same phase simultaneously in the field. An electric potential, also equal, scattered of elating each end of the track is investigated in its own place in the field and beam movement, the number of ions and grains. In field case the ion is given, obviously, by the difference in the two field strengths.

Only tracks taken within a transparent angle in the detector by the (essentially arbitrary) half number $\Theta \approx 15^\circ$, $\phi \approx 15^\circ$ were used in the calculations. Only tracks number of this the pyramid in the direction of the incident beam were counted; the direction of a track within an angle Θ is inferred from the grain density along the track. The proton ionization were locally near the end of the detector of the track.

The ray data, as detailed above, were processed in an IBM 704 computer, which automatically calculated the range

$$R = 2.0 \cos \Theta \sin \phi = 1.7 \cos \psi$$

where ψ is the polar angle, for each track. The range was measured. The ψ angle had a distribution, which was measured. A large-angle scattering from a collimated beam of massive nucleus, the track was measured in the detector portions and the next part of the track was measured. To obtain the total range, the ψ angle is given, obviously,

The table used is that of J. J. Thomson, *Philosophical Magazine*

versus energy for the type K2 emulsion the machine determined the energy of the proton; the energy of the neutron was then found from the relation

$$E_n = E_p / \cos^2 \psi,$$

where all energies are in the laboratory system and the proton and neutron are taken to have the same mass m and non-relativistic velocities. This latter assumption is clearly acceptable in the region investigated, where $E_n \approx 9$ Mev. The relation above follows readily from Hamilton's formula for kinetic energy and the law of conservation of momentum in the laboratory system:

$$E_n = \frac{|\vec{P}_n|^2}{2m}$$

$$|\vec{P}_n| = |\vec{P}_p| \cos \psi + |\vec{P}_{n'}| \sin \psi$$

$$|\vec{P}_p| \sin \psi = |\vec{P}_{n'}| \cos \psi$$

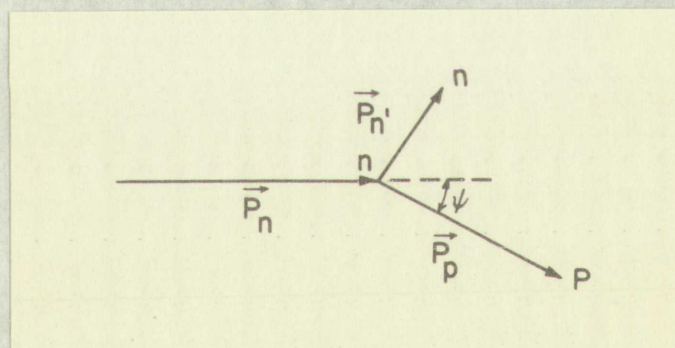


Fig. 4.--An n-p collision

Here E_n is the initial energy of the neutron, P_n the momentum of the incident neutron, E_p the energy of the recoil proton

Relations for Ilford Nuclear Emulsions, A.E.R.E. G/R 664, Harwell, Berks, England (1951). Permission to reproduce this table is not forthcoming.

where E_n is the initial energy of the neutron, E_p the energy of the proton of the incident neutron, E_n' the energy of the neutron, E_p' the energy of the proton after the collision.

$$E_n' = E_n \cos^2 \psi + E_p \sin^2 \psi$$

where all energies are in the laboratory system and the proton and neutron are taken to have the same mass and non-relativistic velocities. This latter assumption is clearly acceptable in the region investigated, where $E_n \approx 5$ eV.

The relation above follows readily from Hamilton's formula for kinetic energy and the law of conservation of momentum in the laboratory system:

$$\begin{aligned} \frac{1}{2} m_n v_n^2 &= \frac{1}{2} m_n v_n'^2 + \frac{1}{2} m_p v_p'^2 \\ \psi \sin \left(\frac{\pi}{2} - \psi \right) + \psi \cos \left(\frac{\pi}{2} - \psi \right) &= \left(\frac{v_n'}{v_n} \right) \sin \left(\frac{\pi}{2} - \psi \right) + \left(\frac{v_p'}{v_n} \right) \cos \left(\frac{\pi}{2} - \psi \right) \\ \psi \cos \left(\frac{\pi}{2} - \psi \right) &= \psi \sin \left(\frac{\pi}{2} - \psi \right) \end{aligned}$$

Fig. 4. -- An n-p collision

where E_n is the initial energy of the neutron, E_p the energy of the proton of the incident neutron, E_n' the energy of the neutron, E_p' the energy of the proton after the collision.

Reproduction for limited distribution. U.S. Gov. Printing Office, Washington, D.C. 20540. This table is not for sale.

and \vec{P}_p its momentum; \vec{P}_n is the momentum of the neutron after the collision. ψ is again the angle, in the laboratory system, between the direction of motion of the recoiling proton and that of the incident neutron. Combining the last two relations,

$$|\vec{P}_n| = |\vec{P}_p| \cos \psi + |\vec{P}_p| \tan \psi \sin \psi,$$

whence

$$E_n = \frac{|\vec{P}_n|^2}{2m} = \frac{|\vec{P}_p|^2}{2m} \frac{1}{\cos^2 \psi} = E_p / \cos^2 \psi.$$

Having performed these calculations, the machine then tabulated the data in order of increasing E_n .

In order to arrive at an expression for the incident flux of neutrons as a function of energy, it is necessary to consider a time-integrated flux $F(E_n \pm \Delta E_n/2)$ of neutrons of energy $E_n \pm \frac{1}{2} \Delta E_n$ incident on a nuclear emulsion of thickness t centimeters containing n hydrogen atoms per cubic centimeter. $F(E_n \pm \frac{1}{2} \Delta E_n)$ is the number of neutrons per square centimeter normal to the flux in the energy range $E_n \pm \frac{1}{2} \Delta E_n$. Let $\sigma_{n-p}(E_n)$ represent the n - p scattering cross section for neutrons of energy E_n , and let $N_p(E_p \pm \frac{1}{2} \Delta E_p)$ be the number of protons measured in the energy interval $E_p \pm \frac{1}{2} \Delta E_p$ corresponding to the energy interval $E_n \pm \frac{1}{2} \Delta E_n$, where $E_p = E_n \cos^2 \psi$, ψ being the laboratory angle between the path of the incident neutron and that of the recoil proton. If Θ be the solid angle of acceptance in the laboratory corresponding to a maximum acceptable angle of α for dip angle ϕ or horizontal angle θ , then Ω , given by

$$\Omega = 16 \sin \alpha \tan^{-1}(\sin \alpha)$$

and \bar{V}

often for a

system, but

proton

fact

$$|\bar{V}| = |\bar{V}'| + |\bar{V}''|$$

where

$$|\bar{V}'| = \dots$$

$$|\bar{V}''| = \dots$$

level

indicated

In

line

consider

of energy

is

is

$E_{H'} = \dots$

normal

represent

energy

measured

the

the

and

of

is

$e = \dots$

$\Omega = \dots$

is the corresponding solid angle in the center of mass system.⁴ Assuming⁵ that n-p scattering is isotropic in the center of mass system, the fraction of tracks which are counted is then

$$\Omega / 4\pi.$$

Let $P(E_p)$ be the correction, to be specified in detail below, for protons of energy E_p leaving the emulsion, and

Handwritten note: H *from proof*

the case in the immediate experiment.

Let, if A be the area (cm^2) of emulsion analyzed,

$$N_p(E_p \pm \frac{1}{2} \Delta E_p) P(E_p) = \frac{F(E_n \pm \frac{1}{2} \Delta E_n) n A t \sigma_{n-p}(E_n) \Omega}{4\pi T(E_n)},$$

from which it is immediate that

$$F(E_n \pm \frac{1}{2} \Delta E_n) = \frac{4\pi}{\Omega \sigma_{n-p}(E_n) n A t} N_p(E_p \pm \frac{1}{2} \Delta E_p) P(E_p) T(E_n).$$

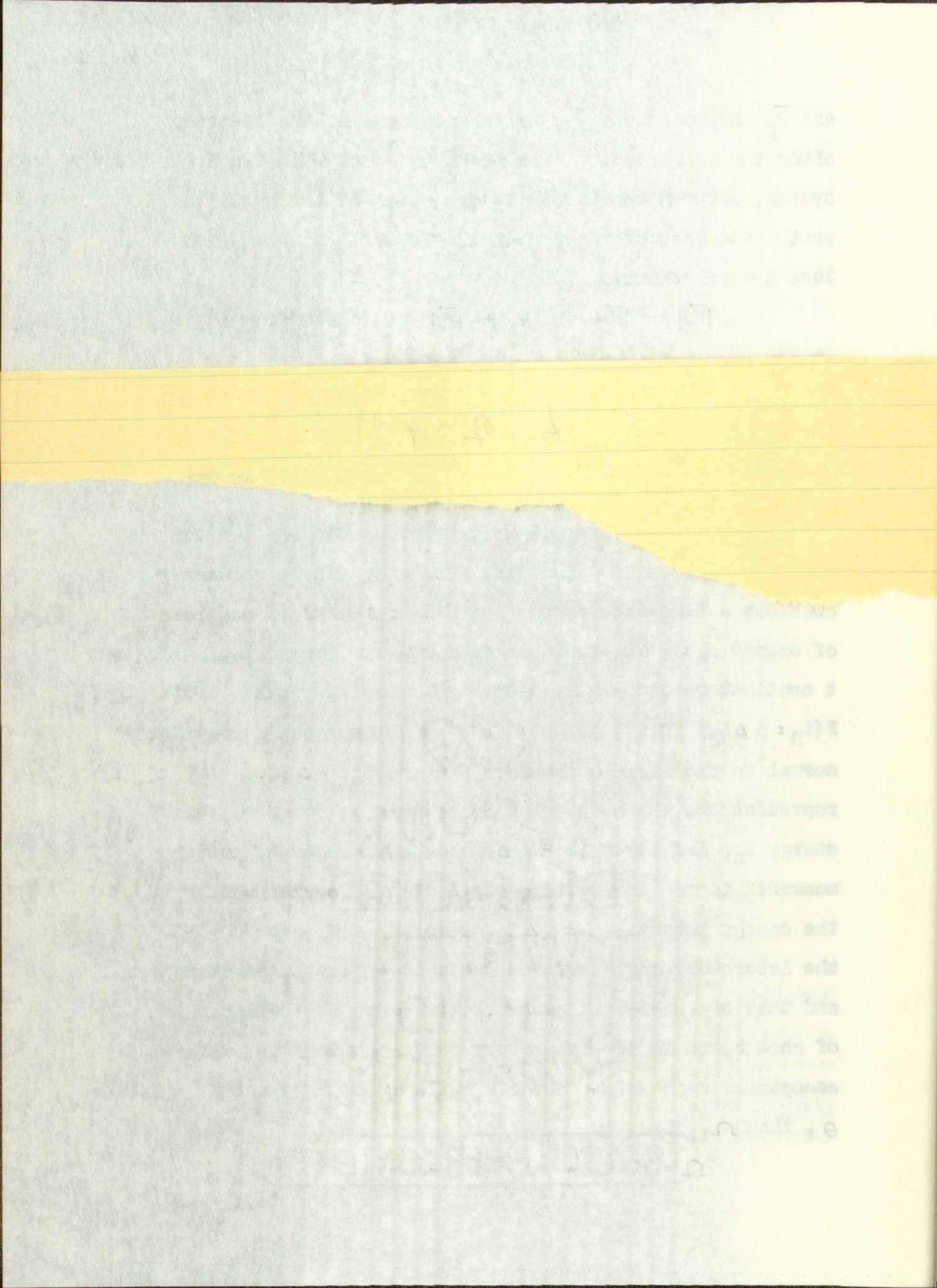
This is the required expression.

The correction $P(E_p)$ for the probability that a track made by a proton of energy E_p will leave the emulsion and hence not be counted may be calculated⁶ on either of the

⁴For the calculation of Ω , see Appendix A.

⁵The n-p scattering process is known to be isotropic in the center of mass system for the energy range considered (0 to 8 Mev) to within 2%. Stephen R. White: "Photographic Plate Detection," in Fast Neutron Physics (New York: Interscience, 1960), I.

⁶The problem is not unrelated to Buffon's needle problem of probability theory.



is the corresponding solid angle in the center of mass system.⁴ Assuming⁵ that n-p scattering is isotropic in the center of mass system, the fraction of tracks which are counted is then

$$\Omega / 4\pi .$$

Let $P(E_p)$ be the correction, to be specified in detail below, for protons of energy E_p leaving the emulsion, and let $T(E_n)$ be the correction for attenuation of the incident neutron beam as it traverses the emulsion. The nuclear emulsion is considered to present an end-on view to the incident flux, as was the case in the immediate experiment. Then one can write, if A be the area (cm^2) of emulsion analyzed,

$$N_p(E_p \pm \frac{1}{2} \Delta E_p) P(E_p) = \frac{F(E_n \pm \frac{1}{2} \Delta E_n) n A t \sigma_{n-p}(E_n) \Omega}{4\pi T(E_n)},$$

from which it is immediate that

$$F(E_n \pm \frac{1}{2} \Delta E_n) = \frac{4\pi}{\Omega \sigma_{n-p}(E_n) n A t} N_p(E_p \pm \frac{1}{2} \Delta E_p) P(E_p) T(E_n).$$

This is the required expression.

The correction $P(E_p)$ for the probability that a track made by a proton of energy E_p will leave the emulsion and hence not be counted may be calculated⁶ on either of the

⁴For the calculation of Ω , see Appendix A.

⁵The n-p scattering process is known to be isotropic in the center of mass system for the energy range considered (0 to 8 Mev) to within 2%. Stephen R. White: "Photographic Plate Detection," in Fast Neutron Physics (New York: Interscience, 1960), I.

⁶The problem is not unrelated to Buffon's needle problem of probability theory.

is the corresponding value in the order of magnitude system. The number of particles in the order of magnitude system is denoted by N .

$$N = \sum_{i=1}^M n_i$$

Let $P(x)$ be the probability density function of the number of particles in the order of magnitude system. The number of particles in the order of magnitude system is denoted by x . The number of particles in the order of magnitude system is denoted by x . The number of particles in the order of magnitude system is denoted by x .

$$P(x) = \frac{1}{N} \sum_{i=1}^M n_i \delta(x - x_i)$$

from which it is evident that

$$P(x) = \frac{1}{N} \sum_{i=1}^M n_i \delta(x - x_i)$$

This is the relative frequency

The correction $P(x)$ for the general case is made by a proper adjustment of the number of particles in the order of magnitude system.

For the determination of the number of particles in the order of magnitude system, it is necessary to know the number of particles in the order of magnitude system. The number of particles in the order of magnitude system is denoted by N .

The number of particles in the order of magnitude system is denoted by N .

following assumptions: (1) an insignificant number of protons undergo multiple scattering, or (2) as many protons are scattered back into the emulsion by a second scattering as are scattered out of the emulsion by a second scattering.⁷ An empirical study based on the forms of 100 actual tracks for emulsions 200 μ thick has been carried out⁸ for maximum dip angles of 10° and 15° , and the extrapolation of these results to a maximum dip angle of 16° was used in the present analysis. Clearly, since the emulsion may be considered infinitely wide in comparison with its depth, it is $R \cos \theta$ (see Fig. 3) and not the true range R which is directly concerned in the probability correction. Employing the range-energy relation and an average value for $\cos \theta$, one can obtain a graph of the fraction of protons which leave the emulsion versus the initial energy of the proton. Let $f(E_p)$ be the fraction of protons of energy E_p leaving the emulsion, and suppose n out of m tracks stay within the emulsion. Then it is clear that

$$m(1 - f(E_p)) = n,$$

or

$$m = \frac{n}{1 - f(E_p)},$$

whence

⁷L. Rosen, op. cit.; H. T. Richards, A Photographic Plate Spectrum of the Neutrons from the Disintegration of Lithium by Deuterons, Phys. Rev. 59, 796-804 (1941).

⁸L. Rosen, op. cit.

Following assumption (1) an arbitrary number of protons undergo multiple scattering, or (2) as many protons are scattered back into the emulsion by a second scattering as are scattered out of the emulsion by a second scattering. An empirical study based on the fact of 100 actual tracks for emulsions 500 μ which has been carried out for various dip angles of 10° and 15° , and the extrapolation of these results to a maximum dip angle of 15° was used in the present analysis. Clearly, since the emulsion may be considered infinitely wide in comparison with the depth, it is $R \cos \theta$ (see Fig. 3) and not the true range R which is directly concerned in the probability calculation. Applying the range-energy relation and an average value for $\cos \theta$, one can obtain a graph of the fraction of protons which leave the emulsion versus the initial energy of the proton. Let $f(E_p)$ be the fraction of protons of energy E_p leaving the emulsion, and suppose n out of n tracks stay within the emulsion. Then it is clear that

$$n(1 - f(E_p)) = n_1$$

$$n = \frac{n_1}{1 - f(E_p)}$$

where

J. Rosen, *ibid.*, p. 11, 1954. A translation of this paper is available from the International Atomic Energy Agency, Vienna, Austria (1954).

J. Rosen, *ibid.*, p. 11.

$$P(E_p) = \frac{1}{1 - T(E_p)}$$

It is then a simple matter, making use of the relation

$$E_n = \overline{E_p} / \overline{\cos^2 \psi},$$

where $\overline{\cos^2 \psi}$ is the "average" value⁹ of $\cos^2 \psi$ over the solid angle considered, to obtain the accompanying graph (Fig. 5) of $P(E_p)$ versus E_n , which is expected to be correct to within 3%.

The values of σ_{n-p} were taken from the compilation of Gammel¹⁰ (partly reproduced in Table 1) and are considered correct to within 2%. The number of hydrogen atoms per cubic centimeter of the emulsion used is known to be 3.43×10^{22} , corresponding to a density of 0.057 gm/cm^3 .¹¹ The correction $T(E_n)$ for attenuation of the neutron beam in traveling through the emulsion is discussed in some detail by Rosen.¹² By limiting the area of emulsion which is examined to a strip near the edge (0.2 to 0.5 centimeters in the present case), this corrective factor may be considered very close to unity.

Evaluation of the errors encountered in the use of photographic plates for detection of neutrons must rest to a great extent on the opinions of microscopists, as many of

⁹See Appendix B.

¹⁰J. L. Gammel: "The n-p Total and Differential Cross Section in the Energy Range 0 to 40 Mev," in Fast Neutron Physics (New York: Interscience), II. Not yet published.

¹¹J. J. Wilkins, op. cit., Fig. 1.

¹²L. Rosen, op. cit.

$$E_{11} = \frac{1}{1 - \cos \psi}$$

It is then a simple matter, using eq. (11), to find

$$E_{11} = \frac{1}{1 - \cos \psi}$$

where $\cos \psi$ is the average value of $\cos \psi$ over the

angle considered, to obtain the average value of E_{11}

of $P(\theta)$ versus θ , which is given in eq. (12) within

limits 3.

The value of $\cos \psi$ over the angle

of interest is given by eq. (13) and the average

correct to within 1%. The value of E_{11} is

able to calculate E_{11} for angles θ in the range

$\theta = 0$ to $\theta = \pi$, corresponding to a scattering angle

correct to within 1% for angles θ in the range

traveling waves, the value of E_{11} is given by

eq. (14) by Rosen, ¹² and is

examined to a high degree of accuracy by

in the present case, with only a few points of

very close to unity.

Discussion of the present results is given in

photographic plates for angles θ in the range

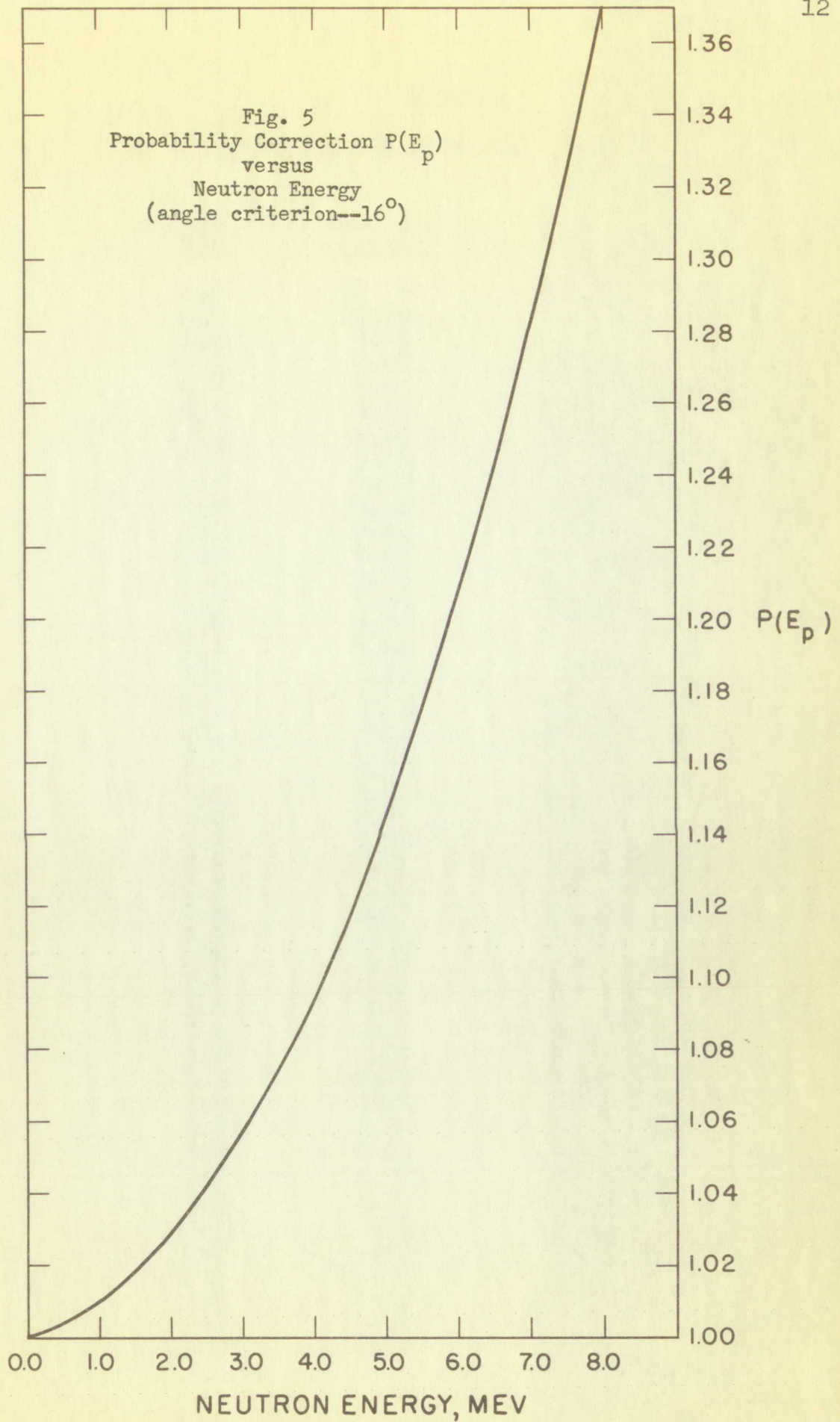
a great extent on the curves in Figures 1 and 2.

¹² See Appendix B.

¹⁰ J. L. Van Dine, *J. Opt. Soc. Am.*, **44**, 101 (1954).

¹¹ Section in the theory of the scattering of light by a

¹² J. L. Van Dine, *J. Opt. Soc. Am.*, **44**, 101 (1954).



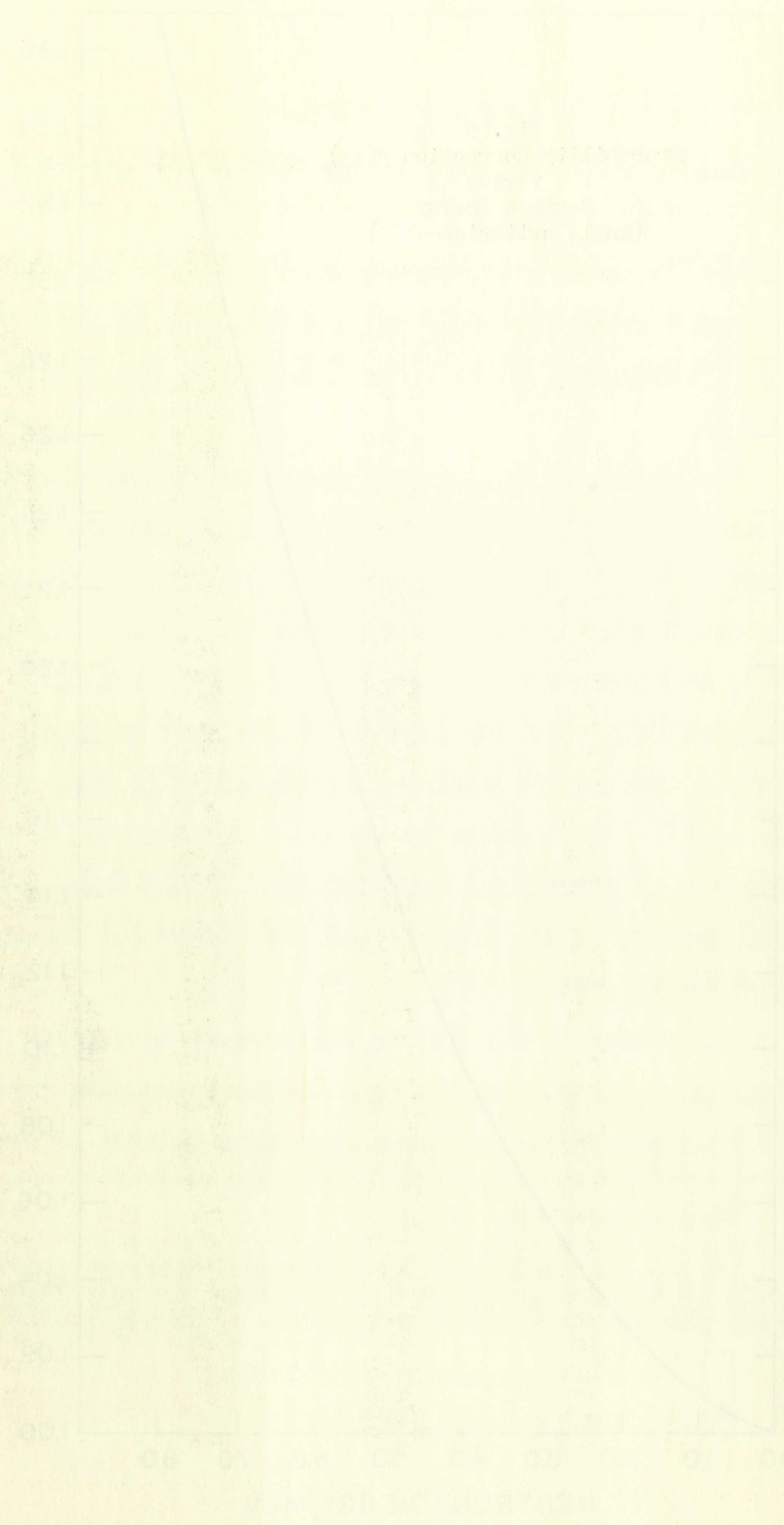
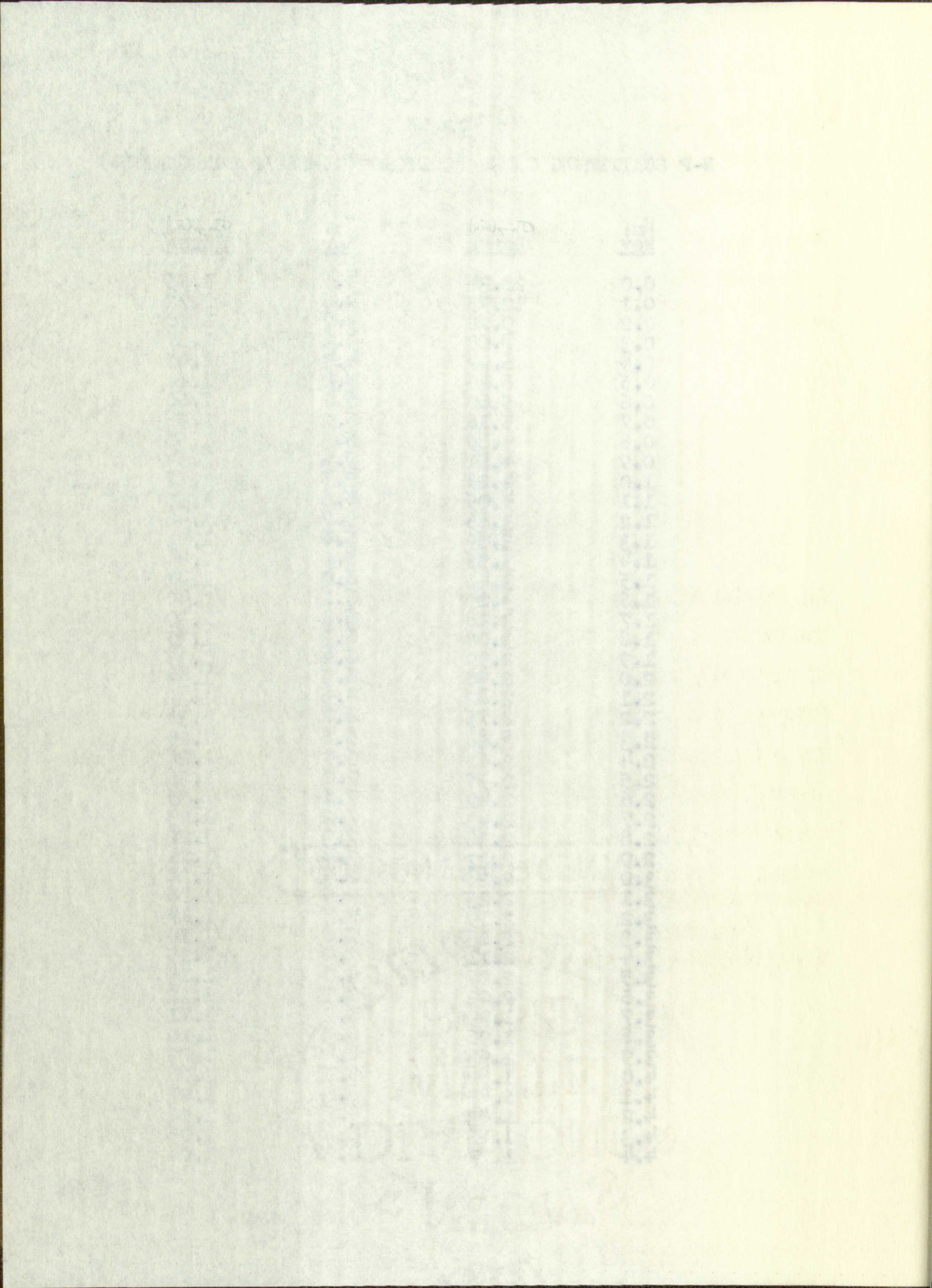


TABLE 1

N-P SCATTERING CROSS SECTIONS (GAMMEL'S FORMULATION)

| E_n , MeV | $\sigma_{n-p}(E_n)$, Barns | E_n , MeV | $\sigma_{n-p}(E_n)$, Barns |
|----------------|--------------------------------|----------------|--------------------------------|
| 0.0 | 20.34 | 4.5 | 1.75 |
| 0.1 | 12.79 | 4.6 | 1.72 |
| 0.2 | 9.70 | 4.7 | 1.70 |
| 0.3 | 8.00 | 4.8 | 1.67 |
| 0.4 | 6.92 | 4.9 | 1.65 |
| 0.5 | 6.16 | 5.0 | 1.62 |
| 0.6 | 5.60 | 5.1 | 1.60 |
| 0.7 | 5.16 | 5.2 | 1.58 |
| 0.8 | 4.80 | 5.3 | 1.56 |
| 0.9 | 4.51 | 5.4 | 1.54 |
| 1.0 | 4.26 | 5.5 | 1.52 |
| 1.1 | 4.05 | 5.6 | 1.50 |
| 1.2 | 3.86 | 5.7 | 1.48 |
| 1.3 | 3.69 | 5.8 | 1.46 |
| 1.4 | 3.55 | 5.9 | 1.44 |
| 1.5 | 3.41 | 6.0 | 1.42 |
| 1.6 | 3.29 | 6.1 | 1.40 |
| 1.7 | 3.18 | 6.2 | 1.39 |
| 1.8 | 3.08 | 6.3 | 1.37 |
| 1.9 | 2.99 | 6.4 | 1.35 |
| 2.0 | 2.90 | 6.5 | 1.34 |
| 2.1 | 2.82 | 6.6 | 1.32 |
| 2.2 | 2.75 | 6.7 | 1.31 |
| 2.3 | 2.68 | 6.8 | 1.29 |
| 2.4 | 2.61 | 6.9 | 1.28 |
| 2.5 | 2.55 | 7.0 | 1.26 |
| 2.6 | 2.49 | 7.1 | 1.25 |
| 2.7 | 2.43 | 7.2 | 1.23 |
| 2.8 | 2.38 | 7.3 | 1.22 |
| 2.9 | 2.33 | 7.4 | 1.21 |
| 3.0 | 2.28 | 7.5 | 1.20 |
| 3.1 | 2.23 | 7.6 | 1.18 |
| 3.2 | 2.19 | 7.7 | 1.17 |
| 3.3 | 2.15 | 7.8 | 1.16 |
| 3.4 | 2.11 | 7.9 | 1.15 |
| 3.5 | 2.07 | 8.0 | 1.13 |
| 3.6 | 2.03 | 8.1 | 1.12 |
| 3.7 | 1.99 | 8.2 | 1.11 |
| 3.8 | 1.96 | 8.3 | 1.10 |
| 3.9 | 1.93 | 8.4 | 1.09 |
| 4.0 | 1.89 | 8.5 | 1.08 |
| 4.1 | 1.86 | 8.6 | 1.07 |
| 4.2 | 1.83 | 8.7 | 1.06 |
| 4.3 | 1.80 | 8.8 | 1.05 |
| 4.4 | 1.77 | 8.9 | 1.04 |



the factors do not permit of more accurate determination. In particular, the accuracy with which the solid angle Θ in the laboratory frame (and hence Ω in the center of mass frame) can be delineated is subject to such uncertainty. Reasonable estimates of the non-statistical errors encountered are:¹³

| | |
|----------------|-----|
| σ_{n-p} | 2% |
| $P(E_p)$ | 3% |
| $T(E_n)$ | 3% |
| n | 5% |
| Ω | 13% |
| t | 3% |

The root-mean-square error is hence 15%. Of these errors, the errors in n and t do not effect the relative distribution of neutrons, and the error in Ω has only a slight effect. (The error in Ω has some effect since Ω is better defined for long than for short tracks because of larger errors in determining horizontal and dip angles for short tracks.) A reasonable estimate of the preciseness with which the relative neutron distribution can be obtained is hence 10%.¹⁴

¹³L. Stewart, Neutron Spectrum and Absolute Yield of a Plutonium-Beryllium Source, Phys. Rev. 98, No. 3, 740-743 (1955).

¹⁴See Rosen, op. cit.

the factors do not permit of any accurate determination. In particular, the accuracy with which the solid angle Ω in the laboratory frame (and hence \bar{v} in the center of mass frame) can be determined is subject to such uncertainty. Reasonable estimates of the non-statistical errors encountered

are:

| | |
|-----------|-----------|
| \bar{v} | $\pm 2\%$ |
| $T(E_n)$ | $\pm 1\%$ |
| $T(E_p)$ | $\pm 1\%$ |
| n | $\pm 1\%$ |
| Ω | $\pm 1\%$ |
| σ | $\pm 1\%$ |

The root-mean-square error is hence 1%. Of these errors, the errors in n and σ do not affect the relative distribution of neutrons, and the error in Ω has only a slight effect. (The error in \bar{v} has some effect since \bar{v} is better defined for long than for short times because of larger errors in determining backward and 45 degree for short times.) A reasonable estimate of the precision with which the relative neutron distribution can be obtained is hence 1%.

J. R. Dunning, Physics Department, University of California, Berkeley, California 94720
 1965 (1965)
 1400 University Ave., Berkeley, Calif.

III. EXPERIMENTAL RESULTS

The IBM tabulation of tracks according to energy of the incident neutron was divided into 0.1 Mev intervals, the number in each energy interval being the $N_p(E_p \pm \frac{1}{2} \Delta E_p)$ defined in the preceding chapter. From Fig. 5 the value of $P(E_p)$ corresponding to the central energy of the interval was found; from Table 1 was obtained the value of $\sigma_{n-p}(E_n)$ for this energy. The time-integrated neutron flux is then proportional to

$$N_p(E_p \pm \frac{1}{2} \Delta E_p) P(E_p) / \sigma_{n-p}(E_n),$$

the constant of proportionality being

$$4\pi / (\Omega n \Delta t).$$

A small area was scanned analyzing all tracks greater than 3μ ; to decrease the statistical uncertainty at high energies without undue expenditure of time, a larger area of the plate was examined with only tracks longer than a set minimum being recorded. Accordingly, the "constant" A (area scanned) was treated as a parameter having the form of a step function.

The flux obtained from the above expression clearly depends on the width of the energy interval considered. To remove this dependence, the flux indicated above was divided by the width ΔE_n of the interval (0.1 Mev). The result is

THE THEORY OF THE ELECTROLYTIC CELL

The EMF of a cell is defined as the potential difference between the two electrodes when no current flows. It is a measure of the maximum work that can be done by the cell in driving a unit quantity of electricity through an external circuit.

$$E = \frac{\Delta G}{nF}$$

The standard EMF of a cell is defined as the EMF of the cell when all the reactants and products are in their standard states. The standard EMF of a cell is a constant at a given temperature and pressure. It is a measure of the standard free energy change of the cell reaction.

The EMF of a cell depends on the standard EMF of the cell and on the activities of the reactants and products. The EMF of a cell is a function of the standard EMF of the cell and of the activities of the reactants and products.

hence in units of neutrons $\text{cm}^{-2}/\text{Mev}$.

After the analysis described above, the data were grouped into larger intervals of energy (to improve statistics) and smoothed. This smoothing is justified since the errors involved in determining the range and angles of a track are large enough to prevent accurate assignment to a 0.1 Mev interval.

Although the background radiation was expected to be low since the critical assembly had been taken out-of-doors and hoisted some thirteen feet above the earth with the emulsions and shield even higher, a portion of a plate exposed to this radiation was analyzed. The neutron flux indicated by this plate was subtracted from the observed spectrum; the correction was of the order of 3% below 1 Mev, 1% from 1 to 2 Mev, 0.8% from 2 to 3 Mev, and less than 0.5% at higher energies.

The leakage neutron spectrum thus obtained for the U^{233} assembly is tabulated in Table 2 with statistical errors and plotted in Fig. 6. The leakage spectra of the structurally similar critical assemblies Godiva (U^{235}) and Jezebel (Pu^{239}) have also been measured¹ using a similar experimental arrangement; these spectra are tabulated in Tables 3 and 4, where the errors shown are the result of counting statistics only.

¹G. M. Frye, Jr., J. H. Gammel, and L. Rosen, Energy Spectrum of Neutrons from Thermal Neutron Fission of U^{235} and from an Untamped Multiplying Assembly of U^{235} (Los Alamos: Los Alamos Scientific Laboratory, 1954), TID-10073; L. Stewart, Leakage Neutron Spectrum from a Bare Pu^{239} Critical Assembly, Nuclear Sci. and Eng. E, 596 (1960).

hence in units of cm^{-1} ...
After the analysis ...
grouped into ...
and associated ...
involved in ...
large amount of ...
interval.

Although the ...
low since the critical ...
and related ...
excitation and ...
to this radiation ...
by this phase ...
correction was ...
2 Nov, 1955 ...
checked.

The ...
U235 assembly ...
and placed in ...
other critical ...
have also been ...
these spectra ...
errors shown ...

10. H. ...
...
...
...
...

CONFIDENTIAL

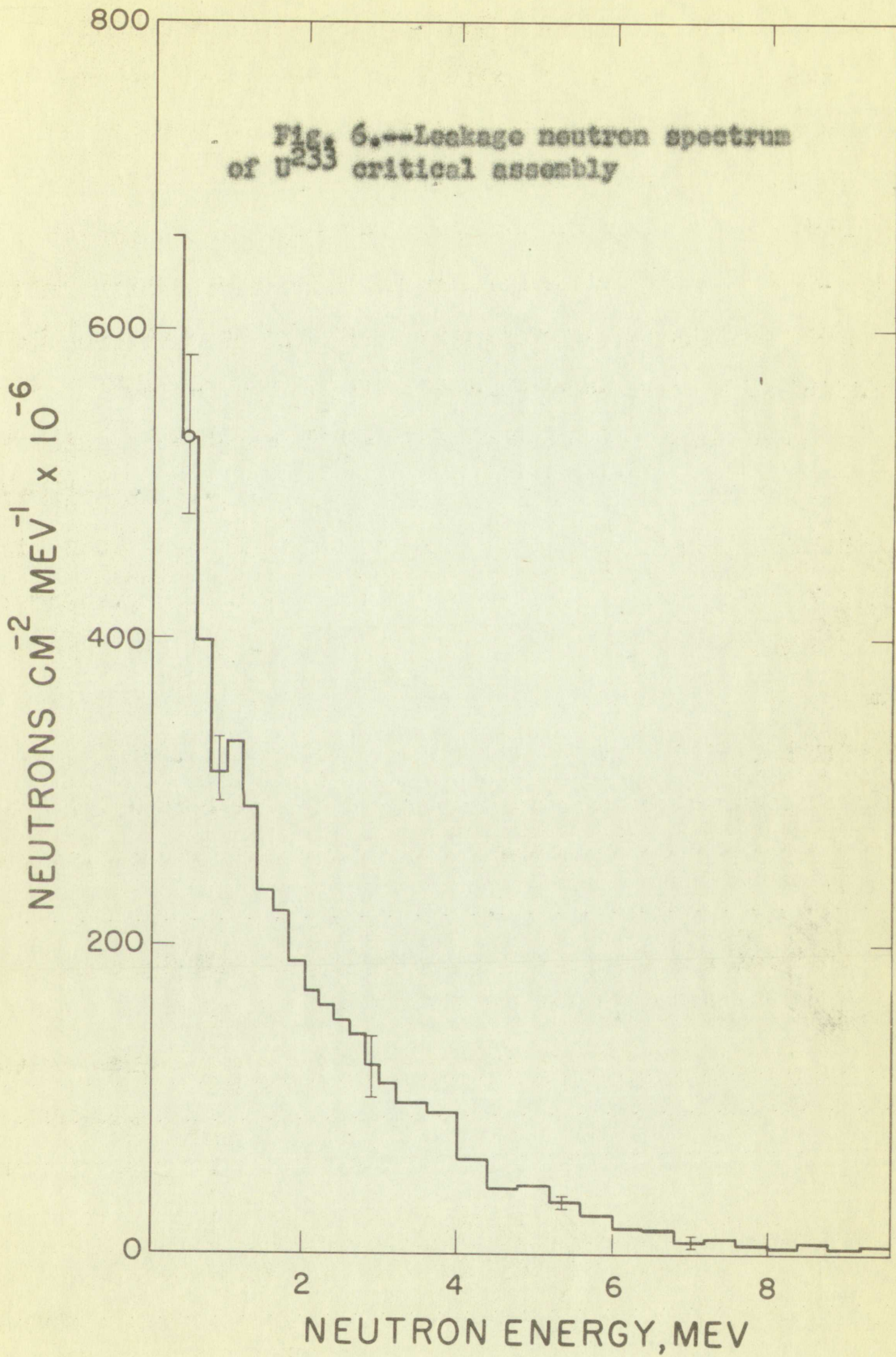
TABLE 2
Leakage Neutron Spectrum of Jezebel U²³³

| Neutron Energy Interval, MeV | Neutrons/cm ² per MeV | Statistical Uncertainty, % | Neutron Energy Interval, MeV | Neutrons/cm ² per MeV | Statistical Uncertainty, % |
|------------------------------|----------------------------------|----------------------------|------------------------------|----------------------------------|----------------------------|
| --- | --- | -- | 3.2 - 3.6 | 94.3 x 10 ⁶ | 9 |
| 0.3 - 0.4 | 646 x 10 ⁶ | 11 | 3.6 - 4.0 | 83.6 | 10 |
| 0.4 - 0.6 | 520 | 10 | 4.0 - 4.4 | 57.9 | 12 |
| 0.6 - 0.8 | 391 | 7 | 4.4 - 4.8 | 41.6 | 14 |
| 0.8 - 1.0 | 306 | 7 | 4.8 - 5.2 | 42.6 | 15 |
| 1.0 - 1.2 | 324 | 8 | 5.2 - 5.6 | 32.3 | 15 |
| 1.2 - 1.4 | 299 | 8 | 5.6 - 6.0 | 23.5 | 22 |
| 1.4 - 1.6 | 230 | 10 | 6.0 - 6.4 | 14.3 | 30 |
| 1.6 - 1.8 | 209 | 11 | 6.4 - 6.8 | 13.6 | 30 |
| 1.8 - 2.0 | 182 | 10 | 6.8 - 7.2 | 6.0 | 50 |
| 2.0 - 2.2 | 166 | 10 | 7.2 - 7.6 | 8.4 | 40 |
| 2.2 - 2.4 | 157 | 10 | 7.6 - 8.0 | 4.4 | 60 |
| 2.4 - 2.6 | 148 | 10 | 8.0 - 8.4 | 1.7 | 100 |
| 2.6 - 2.8 | 138 | 10 | 8.4 - 8.8 | 5.2 | 60 |
| 2.8 - 3.0 | 119 | 11 | 8.8 - 9.2 | 2.5 | 90 |
| 3.0 - 3.2 | 108 | 12 | 9.2 - 9.6 | 3.1 | 80 |

| Localities | No. of persons | No. of persons | No. of persons | No. of persons | No. of persons |
|--------------|----------------|----------------|----------------|----------------|----------------|
| [Faint text] | [Faint text] | [Faint text] | [Faint text] | [Faint text] | [Faint text] |
| [Faint text] | [Faint text] | [Faint text] | [Faint text] | [Faint text] | [Faint text] |
| [Faint text] | [Faint text] | [Faint text] | [Faint text] | [Faint text] | [Faint text] |

Table showing the number of persons in each locality

5



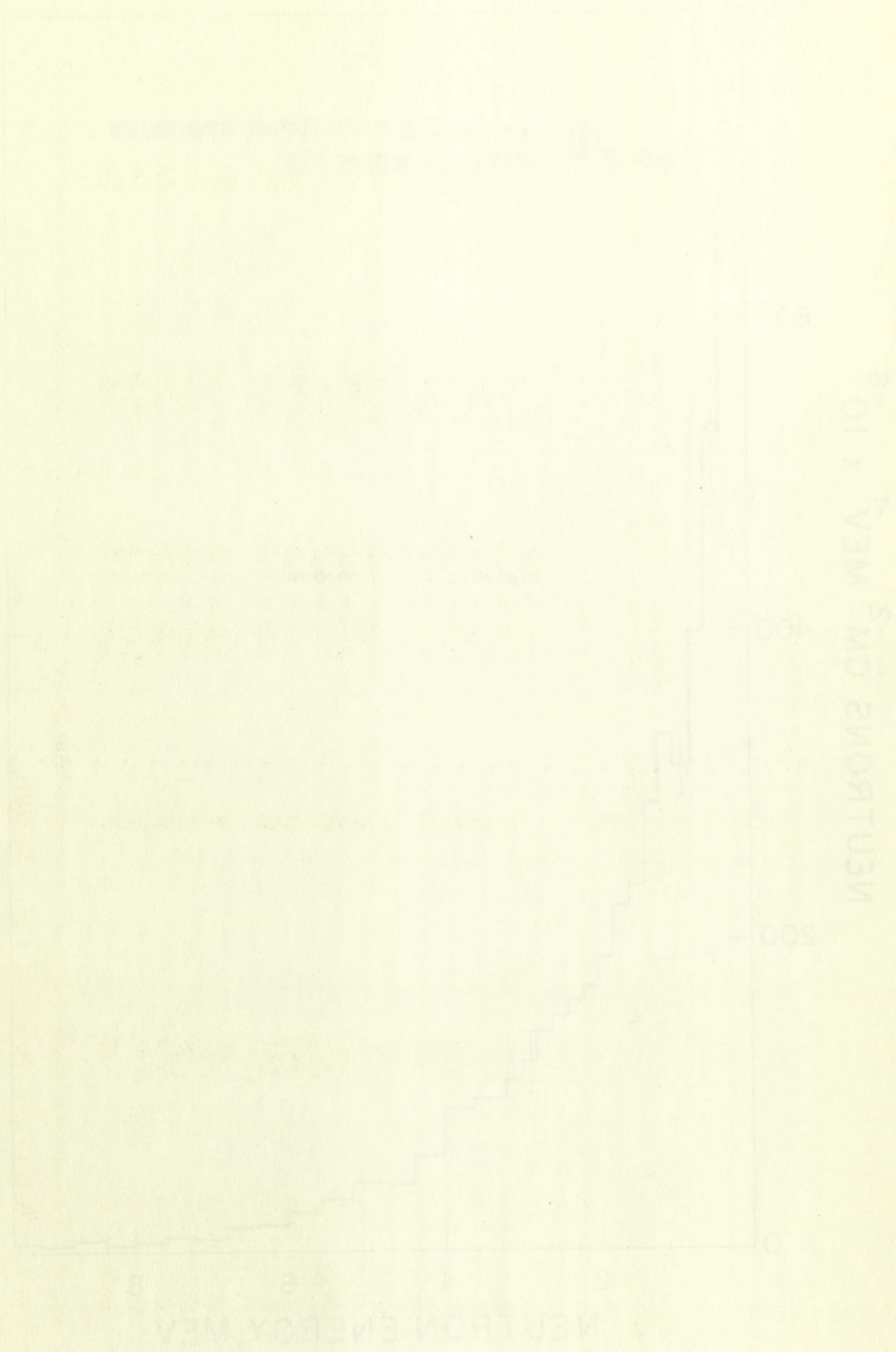


TABLE 3

LEAKAGE NEUTRON SPECTRUM OF GODIVA U²³⁵^a

| Neutron Energy Interval, Mev | Neutrons/cm ² per Mev | Statistical Uncertainty, % | Neutron Energy Interval, Mev | Neutrons/cm ² per Mev | Statistical Uncertainty, % |
|------------------------------|----------------------------------|----------------------------|------------------------------|----------------------------------|----------------------------|
| 0.2 - 0.4 | 721 x 10 ⁵ | 4 | 3.0 - 3.4 | 84.6 x 10 ⁵ | 9 |
| 0.4 - 0.6 | 718 | 3 | 3.4 - 3.8 | 70.5 | 8 |
| 0.6 - 0.8 | 612 | 4 | 3.8 - 4.2 | 62.1 | 9 |
| 0.8 - 1.0 | 499 | 4 | 4.2 - 4.6 | 40.7 | 11 |
| 1.0 - 1.2 | 371 | 5 | 4.6 - 5.0 | 42.9 | 11 |
| 1.2 - 1.4 | 320 | 6 | 5.0 - 5.4 | 33.6 | 14 |
| 1.4 - 1.6 | 257 | 7 | 5.4 - 5.8 | 21.7 | 16 |
| 1.6 - 1.8 | 218 | 8 | 5.8 - 6.2 | 12.9 | 24 |
| 1.8 - 2.0 | 224 | 8 | 6.2 - 6.6 | 10.8 | 27 |
| 2.0 - 2.2 | 193 | 7 | 6.6 - 7.0 | 11.4 | 27 |
| 2.2 - 2.4 | 159 | 8 | 7.0 - 7.4 | 13.9 | 25 |
| 2.4 - 2.6 | 141 | 9 | 7.4 - 7.8 | 1.9 | 70 |
| 2.6 - 2.8 | 122 | 9 | 7.8 - 8.2 | 2.2 | 70 |
| 2.8 - 3.0 | 136 | 9 | 8.2 - 8.6 | 6.6 | 40 |
| | | | 8.6 - 9.0 | 2.4 | 70 |

^aTable from Frye, et. al., op. cit.

BOARD

MEMBERS

| NAME | RESIDENCE | EDUCATION | PROFESSION | BUSINESS | MEMBERSHIP |
|--------------|-----------|-----------|------------|----------|------------|
| 1. J. W. ... | ... | ... | ... | ... | ... |
| 2. ... | ... | ... | ... | ... | ... |
| 3. ... | ... | ... | ... | ... | ... |
| 4. ... | ... | ... | ... | ... | ... |
| 5. ... | ... | ... | ... | ... | ... |
| 6. ... | ... | ... | ... | ... | ... |
| 7. ... | ... | ... | ... | ... | ... |
| 8. ... | ... | ... | ... | ... | ... |
| 9. ... | ... | ... | ... | ... | ... |
| 10. ... | ... | ... | ... | ... | ... |
| 11. ... | ... | ... | ... | ... | ... |
| 12. ... | ... | ... | ... | ... | ... |
| 13. ... | ... | ... | ... | ... | ... |
| 14. ... | ... | ... | ... | ... | ... |
| 15. ... | ... | ... | ... | ... | ... |
| 16. ... | ... | ... | ... | ... | ... |
| 17. ... | ... | ... | ... | ... | ... |
| 18. ... | ... | ... | ... | ... | ... |
| 19. ... | ... | ... | ... | ... | ... |
| 20. ... | ... | ... | ... | ... | ... |

MEMBER RESIDENCE REGISTER OF COUNTY A 532

TABLE 4
LEAKAGE NEUTRON SPECTRUM OF JEJEBEL Pu 239^a

| Neutron Energy Interval, Mev | Neutrons/cm ² per Mev | Neutron Energy Interval, Mev | Neutrons/cm ² per Mev |
|------------------------------|----------------------------------|------------------------------|----------------------------------|
| 0.3 - 0.5 | (289 ± 14) × 10 ⁶ | 3.5 - 3.9 | (50.3 ± 5.2) × 10 ⁶ |
| 0.5 - 0.7 | 250 ± 14 | 3.9 - 4.3 | 44.0 ± 5.0 |
| 0.7 - 0.9 | 224 ± 14 | 4.3 - 4.7 | 33.9 ± 4.5 |
| 0.9 - 1.1 | 177 ± 13 | 4.7 - 5.1 | 28.8 ± 4.3 |
| 1.1 - 1.3 | 176 ± 12 | 5.1 - 5.5 | 16.6 ± 3.3 |
| 1.3 - 1.5 | 164 ± 13 | 5.5 - 5.9 | 16.5 ± 3.4 |
| 1.5 - 1.7 | 152 ± 12 | 5.9 - 6.3 | 8.2 ± 2.5 |
| 1.7 - 1.9 | 125 ± 11 | 6.3 - 6.7 | 11.2 ± 3.0 |
| 1.9 - 2.1 | 122 ± 12 | 6.7 - 7.1 | 9.7 ± 2.9 |
| 2.1 - 2.3 | 96.1 ± 8.4 | 7.1 - 7.5 | 4.7 ± 2.1 |
| 2.3 - 2.5 | 87.0 ± 8.2 | 7.5 - 7.9 | 4.3 ± 2.1 |
| 2.5 - 2.7 | 85.7 ± 8.3 | 7.9 - 8.3 | 2.1 ± 1.5 |
| 2.7 - 3.1 | 70.1 ± 5.6 | 8.3 - 8.7 | 4.9 ± 2.5 |
| 3.1 - 3.5 | 61.5 ± 5.5 | 8.7 - 9.1 | 1.2 ± 1.2 |

^aTable from Stewart, Leakage Neutron Spectrum.

| SPECIAL INVESTIGATION | No. of cases investigated | Percentage of cases investigated | Total number of cases |
|-----------------------|---------------------------|----------------------------------|-----------------------|
| 1. ... | ... | ... | ... |
| 2. ... | ... | ... | ... |
| 3. ... | ... | ... | ... |
| 4. ... | ... | ... | ... |

REPORT ON THE INVESTIGATION OF ...

For Fig. 7 the three spectra have been normalized so that the area under each curve from 0.3 to 9.5 Mev is the same. The figure shows² that the leakage spectra of the U²³³ and Pu²³⁹ assemblies are quite similar and that both are "harder" than that of the U²³⁵ assembly. By being "harder" is meant having relatively more high-energy neutrons. These observations are in keeping with the known cross sections and fission spectra of these elements.

The discontinuity at 1.1 Mev is of questionable significance since the statistical uncertainties are fairly large in this region. Note, however, that there is an indication of such a discontinuity at the same energy in the Pu²³⁹ spectrum. Possibly some resonance phenomenon is indicated.

²See also Table 6 of the following chapter.

For Fig. 7 the three spectra have been normalized so that the area under each curve from 0.5 to 2.5 Mev is the same. The figure shows that the average spectra of the U^{233} and U^{235} assemblies are quite similar and that both are "borderline" in nature, that is of the U^{235} assembly, by being "borderline" in nature having relatively more high-energy neutrons. These observations are in keeping with the known cross sections and fusion spectra of these elements.

The discontinuity at 1.1 Mev is of questionable significance since the statistical uncertainties are fairly large in this region. However, it is noted that there is an indication of such a discontinuity at the same energy in the U^{235} spectrum. Possibly some resonance phenomenon is indicated.

See also Table 6 of the following paper.

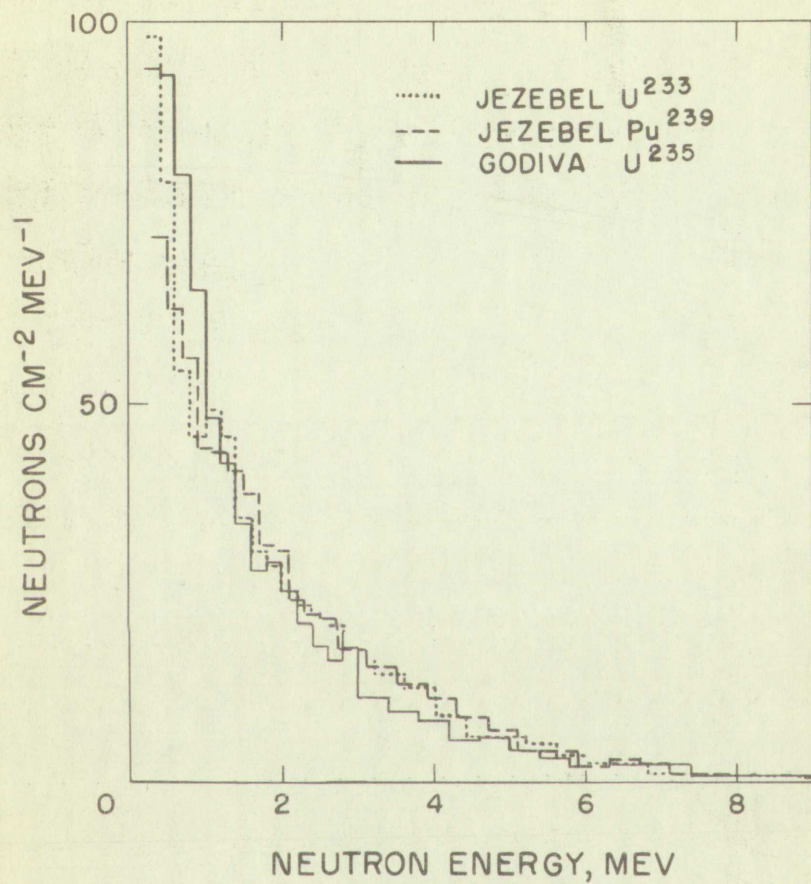


Fig. 7.--Leakage neutron spectra of three critical assemblies

Figure 1. Neutron energy spectrum of the reactor.

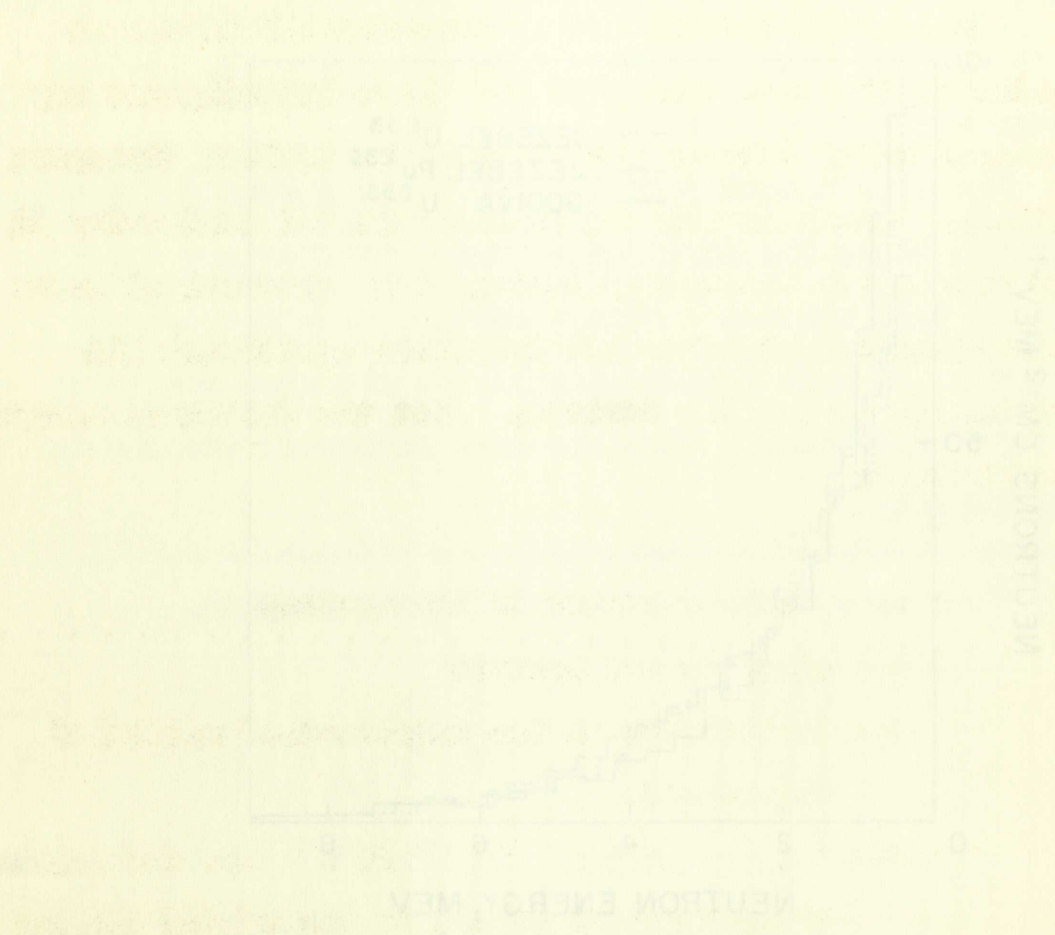


Fig. 1. Neutron energy spectrum of the reactor.

IV. APPLICATION OF THE NEUTRON TRANSPORT EQUATION TO SPHERICAL CRITICAL ASSEMBLIES

The leakage spectrum of so structurally simple an assembly as the bare sphere of U^{233} here investigated may be determined by solving numerically the neutron transport equation. Assuming for the moment that all scattering is isotropic in the laboratory system, the mathematical form of the transport equation (or Boltzmann equation)¹ for neutrons may be readily derived. Let the following definitions be laid down:

t --- time

\vec{r} --- position vector of the neutron

v --- speed of the neutron

\vec{n} --- unit vector in the direction of motion of the neutron

$n \, dV \, dv \, d\Omega \equiv n(\vec{r}, v, \vec{n}, t) \, dV \, dv \, d\Omega$ --- the number of neutrons at time t in the volume element dV around the point defined by \vec{r} having a speed between v and $v + dv$ in a direction lying within a differential solid angle $d\Omega$ about the direction \vec{n}

¹For the general form of this equation see E. Davison: Neutron Transport Theory (Oxford: At the Clarendon Press, 1957), pp. 15-16, on which the present development is based.

IV. THE THEORY OF THE ...

The theory of the ... is based on the ... of the ... and the ... of the ...

The ... is defined as ... and the ... is defined as ...

The ... is defined as ... and the ... is defined as ...

The ... is defined as ... and the ... is defined as ...

$S dV dv d\Omega dt = S(\vec{r}, v\vec{n}, t) dV dv d\Omega dt$ --- the number of neutrons having speed between v and $v + dv$ and moving in a direction within the differential solid angle $d\Omega$ about the direction \vec{n} arising in dV in the time dt due² to both fission and scattering.

Consider a packet of neutrons with velocity $v\vec{n}$ and position $\vec{r} + tv\vec{n}$ at times close to $t = 0$. Then the net increase in the number of neutrons in this packet is, by definition,

$$\frac{dn}{dt} dV dv d\Omega dt$$

as t increases by dt .

It is clear that neutrons may be removed from the packet by capture and by scattering out of the packet. Since a neutron which undergoes a scattering process must change either speed or direction of travel, for otherwise no scattering can be said to have taken place, and since the probability that a neutron emitted during fission will have the same speed and direction as the neutron causing the fission is of the second order in small quantities, decrease of the number of neutrons in the packet in time dt due to scattering and capture (with or without subsequent fission) is simply the number of neutrons undergoing collisions in the time dt . Using $\sigma(v)$ for the total probability of

²It is assumed herein that no sources independent of the neutron flux are present. This assumption implies, among other considerations, that spontaneous fission is negligible.

217
position T + ...
increase in the ...
distortion,
as it increases by ...
It is clear that ...
packed by ...
Since a ...
change also ...
no scattering ...
probability ...
the same ...
fraction is ...
of the number ...
scattering ...
is simply ...
the time ...

It is ...
the number ...
every ...
negligible

collision for neutrons of velocity v , it is clear that the decrease in time dt due to these causes is given by

$$\sigma(v) n v dV dv d\Omega dt,$$

where nv is the number of neutrons passing through unit area perpendicular to \vec{n} per second and $n v dV dv d\Omega dt$ is hence the number passing through dV in time dt . Here, and throughout this section, σ will be assumed to be in units of cm^{-1} ; i. e., obtained from the conventional cross section (cm^2) by multiplying this cross section by the number of nuclei per cm^3 of the element considered. Thus σ as used here is the reciprocal of the mean free path.

The increase in the number of neutrons in the packet due to scattering into the packet is due to collisions occurring in dV , and similarly the increase due to fission is due to fissioning atoms lying in dV . Hence this increase is

$$S(\vec{r}, v\vec{n}, t) dV dv d\Omega dt.$$

Recalling from vector analysis that

$$\frac{dn}{dt} = D_t n + v\vec{n} \cdot \nabla n,$$

collecting results, and cancelling differentials, there results the expression

$$D_t n + v\vec{n} \cdot \nabla n + \sigma(v)nv = S(\vec{r}, v\vec{n}, t)$$

for neutron balance: the net rate of increase of neutrons in the given packet plus the number of neutrons lost from the packet per second equals the rate at which neutrons are created in the packet. For a time-independent problem such as that considered,

collision for neutrons of velocity v is clear that the decrease in time dt due to these causes is given by

$$d\tau = n v dt \Omega$$

where n is the number of neutrons passing through unit area perpendicular to \vec{n} per second and $v dt \Omega$ is the volume swept out by the neutron passing through dv in time dt . Here, and throughout this section, τ will be assumed to be in units of cm^{-1} . $i.e.$, obtained from the conventional cross section (σ) by multiplying this cross section by the number of nuclei per unit volume. Thus τ as used here is the reciprocal of the mean free path.

The increase in the number of neutrons in the packet due to scattering into the packet is due to collisions occurring in dv , and similarly the decrease due to fission is due to fissioning neutrons lying in dv . Hence this increase is

$$dN = N dv \Omega$$

Recalling from vector analysis that

$$\nabla \cdot \vec{n} = \frac{1}{r^2} \frac{d}{dr} (r^2 n_r)$$

collecting results, and cancelling differentials, there results the expression

$$\frac{dN}{dt} = N dv \Omega + \nabla \cdot \vec{n} N dv$$

For neutron balance the net rate of increase of neutrons in the given packet plus the number of neutrons lost from the packet per second equals the rate at which neutrons are added in the packet. For a time-independent problem, and as that considered,

$$v \vec{\Omega} \cdot \nabla n + \sigma(v)nv = S(\vec{r}, v\vec{\Omega}).$$

Assuming³ that all processes involved in S are isotropic in the laboratory frame, and further restricting the discussion to a system possessing spherical symmetry ($\vec{r} \rightarrow r$), one has

$$v \vec{\Omega} \cdot \nabla n(r, v\vec{\Omega}) + \sigma(v)n(r, v\vec{\Omega})v = S(r, v).$$

Since v is a constant scalar, one can write this as

$$\vec{\Omega} \cdot \nabla (vn(r, v\vec{\Omega})) + \sigma(v)vn(r, v\vec{\Omega}) = S(r, v).$$

Introducing the angular neutron flux

$$N(r, v\vec{\Omega}) dV dv d\Omega \equiv v n(r, v\vec{\Omega}) dV dv d\Omega,$$

i.e., the number of neutrons in the volume dV having speeds between v and $v + dv$ and directions of travel within the differential solid angle $d\Omega$ about Ω passing through one square centimeter perpendicular to Ω per second, the transport equation becomes

$$\vec{\Omega} \cdot \nabla N(r, v\vec{\Omega}) + \sigma(v)N(r, v\vec{\Omega}) = S(r, v).$$

In order to put this equation into the multigroup form, one considers G (arbitrary) energy groups $1, 2, \dots, G, \dots, G$ and integrates the equation over the values of v in each energy group. For group g the transport equation thus takes the form

$$\vec{\Omega} \cdot \nabla N_g(r, \vec{\Omega}) + \sigma_g N_g(r, \vec{\Omega}) = S_g(r),$$

where $N_g(r, \vec{\Omega})$ is the flux in direction $\vec{\Omega}$ of neutrons belonging to the g^{th} group and $S_g(r)$ is the source term for neutrons with energies lying in the g^{th} velocity group:

³A discussion of the validity of this assumption may be found in Davison, *op. cit.*, Chapter 1. See also below for the case of elastic scattering.

$$\nabla \cdot \tilde{N} = \tilde{N} \cdot \nabla + \sigma(\tilde{N})$$

Assuming that all processes involve a finite number of particles, the laboratory frame, and further assuming that the interaction to a system consisting of a finite number of particles...

$$\nabla \cdot \tilde{N} = \tilde{N} \cdot \nabla + \sigma(\tilde{N})$$

Since \tilde{N} is a constant vector, one can write this as

$$\nabla \cdot \tilde{N} = \tilde{N} \cdot \nabla + \sigma(\tilde{N})$$

Introducing the angular momentum...

$$\tilde{N} \cdot \nabla = \nabla \cdot \tilde{N} + \sigma(\tilde{N})$$

i.e., the number of particles in the volume V having spins between ν and $\nu + d\nu$ and direction of travel within the differential solid angle $d\Omega$ about \hat{n} passing through the square surface perpendicular to \hat{n} per second, the group...

part equation becomes

$$\nabla \cdot \tilde{N} = \tilde{N} \cdot \nabla + \sigma(\tilde{N})$$

In order to put this equation into the relativistic form, one considers...

..., and integrates the equation over the volume of V . In each energy group, the group velocity equation may be taken the form

$$\tilde{N} \cdot \nabla = \nabla \cdot \tilde{N} + \sigma(\tilde{N})$$

where $\tilde{N}_g(\nu, \hat{n})$ is the flux in direction \hat{n} of neutrons belonging to the g group and $\nu(\hat{n})$ is the neutron velocity neutrons with energies lying in the g velocity group.

A discussion of the value of $\sigma(\tilde{N})$ and its dependence on \tilde{N} is found in Levin, et al., op. cit., and below for the case of elastic scattering.

$$N_g(\mathbf{r}, \vec{\Omega}) \equiv \int_{V_g} N(\mathbf{r}, \mathbf{v}, \vec{\Omega}) d\mathbf{v},$$

$$S_g(\mathbf{r}) \equiv \int_{V_g} S(\mathbf{r}, \mathbf{v}) d\mathbf{v},$$

$$\sigma_g \equiv \frac{1}{\Delta V_g} \int_{V_g} \sigma(\mathbf{v}) d\mathbf{v},$$

where \int_{V_g} indicates integration over all velocities belonging in group g . Further simplification is possible when the angular neutron flux depends only on the radial coordinate r and the angle between \mathbf{r} and the direction $\vec{\Omega}$ of the flux. Since the cosine of this angle is

$$\mu \equiv \frac{\vec{\mathbf{r}} \cdot \vec{\Omega}}{r},$$

one can replace $N(\mathbf{r}, \vec{\Omega})$ by

$$N(\mathbf{r}, \mu) = N(\mathbf{r}, \frac{\vec{\mathbf{r}} \cdot \vec{\Omega}}{r}).$$

In terms of the variables r and μ one has for the first term in the transport equation

$$\vec{\Omega} \cdot \nabla N(\mathbf{r}, \frac{\vec{\mathbf{r}} \cdot \vec{\Omega}}{r}) = \mu D_r N + (D_\mu N) \vec{\Omega} \cdot \nabla (\frac{\vec{\mathbf{r}} \cdot \vec{\Omega}}{r}).$$

Using well-known vector identities the gradient in the last term can be expanded as

$$\begin{aligned} \nabla (\frac{\vec{\mathbf{r}} \cdot \vec{\Omega}}{r}) &= \frac{1}{r} \nabla (\vec{\mathbf{r}} \cdot \vec{\Omega}) - \frac{1}{r^2} (\vec{\mathbf{r}} \cdot \vec{\Omega}) \nabla r \\ &= \frac{1}{r} \{ \vec{\mathbf{r}} \times (\nabla \times \vec{\Omega}) + \vec{\Omega} \times (\nabla \times \vec{\mathbf{r}}) + (\vec{\mathbf{r}} \cdot \nabla) \vec{\Omega} \\ &\quad + (\vec{\Omega} \cdot \nabla) \vec{\mathbf{r}} \} - \frac{1}{r^2} (\vec{\mathbf{r}} \cdot \vec{\Omega}) \frac{\vec{\mathbf{r}}}{r} \\ &= \frac{1}{r} (\vec{\Omega} \cdot \nabla) \vec{\mathbf{r}} - \frac{1}{r^3} (\vec{\mathbf{r}} \cdot \vec{\Omega}) \vec{\mathbf{r}}, \end{aligned}$$

$$\int_{\nu} W(\mathbf{r}, \mathbf{v}) d\nu = (\mathbf{r}, \mathbf{n}) S$$

$$\int_{\nu} S(\mathbf{r}, \mathbf{v}) d\nu = (\mathbf{r}) S$$

$$\int_{\nu} \frac{1}{\Delta} d\nu = \Delta$$

where \int_{ν} indicates integration over all velocities belonging to group ν . Further simplification is possible when the angular neutron flux depends only on the radial coordinate r and the angle between \mathbf{r} and the direction \mathbf{n} of the flux. Since the cosine of this angle is

$$\mu = \frac{\mathbf{r} \cdot \mathbf{n}}{r}$$

one can replace $W(\mathbf{r}, \mathbf{n})$ by

$$W(\mathbf{r}, \mu) = W(r, \frac{\mathbf{r} \cdot \mathbf{n}}{r})$$

In terms of the variables r and μ one has for the first term in the transport equation

$$\mathbf{n} \cdot \nabla W(\mathbf{r}, \mu) = \frac{\partial W}{\partial r} (\mathbf{n} \cdot \mathbf{r}) + \frac{\partial W}{\partial \mu} (\mathbf{n} \cdot \nabla \mu)$$

Using well-known vector identities the gradient in the last term can be expanded as

$$\nabla \mu = \frac{\nabla(\mathbf{r} \cdot \mathbf{n})}{r} - (\mathbf{n} \cdot \nabla) \frac{\mathbf{r}}{r}$$

$$= \frac{\mathbf{n}(\nabla \cdot \mathbf{r}) + (\nabla \times \mathbf{r}) \times \mathbf{n} + (\mathbf{n} \times \nabla) \times \mathbf{r}}{r}$$

$$= \frac{\mathbf{n}(\nabla \cdot \mathbf{r})}{r} - \frac{\mathbf{r}(\nabla \cdot \mathbf{n})}{r}$$

$$= \frac{\nabla(\mathbf{n} \cdot \mathbf{r})}{r} - \frac{\mathbf{r}(\nabla \cdot \mathbf{n})}{r}$$

since \vec{n} is a constant vector and

$$\nabla \times \vec{r} = 0,$$

\vec{r} being a position vector. Thus

$$\begin{aligned} \vec{n} \cdot \nabla N(r, \mu) &= \mu D_r N + \left(\frac{1}{r} \vec{n} \cdot \vec{n} - \frac{(r \cdot \vec{n})^2}{r^3} \right) D_\mu N \\ &= \mu D_r N + \frac{1 - \mu^2}{r} D_\mu N, \end{aligned}$$

and the transport equation for the problem considered assumes the form

$$\left(\mu D_r + \frac{1 - \mu^2}{r} D_\mu + \sigma_g \right) N_g(r, \mu) = S_g(r).$$

σ_g , the total cross section for the removal of a neutron from the g^{th} group, is obviously given by

$$\sigma_g = \sigma_g^e + \sigma_g^i + \sigma_g^a + \sigma_g^f,$$

where σ_g^e is the cross section for elastic scattering, σ_g^i that for inelastic scattering, σ_g^f the cross section for capture followed by fission, and σ_g^a the cross section for capture followed by any other process, all for neutrons in the velocity group g . When corrected for anisotropic scattering in the manner noted below, σ_g is known as the transport cross section.

It is now necessary to examine in detail the source term $S_g(r)$, in which are included all sources of neutrons in velocity group g , whether from fission or from scattering from another or the same⁴ group. $S_g(r)$ may clearly be written in the standard form

⁴The present consideration must be carefully distinguished from that of the discussion on page 24.

since \bar{n} is a constant vector and

$$\nabla \times \bar{n} = 0,$$

\bar{n} being a position vector. Thus

$$\bar{n} \cdot \nabla \bar{n}(\bar{n} \cdot \nabla) = \frac{1}{2} \nabla^2 \bar{n} + \frac{1}{2} \nabla \nabla^2 \bar{n} = \frac{1}{2} \nabla^2 \bar{n} + \frac{1}{2} \nabla \nabla^2 \bar{n}$$

$$= \frac{1}{2} \nabla^2 \bar{n} + \frac{1}{2} \nabla \nabla^2 \bar{n}$$

and the transport equation for the neutron concentration becomes

the form

$$\left(\frac{1}{v} \frac{d}{dt} + \frac{1}{2} \nabla^2 \right) n + \sigma_a n = S_0(r).$$

where σ_a is the total cross section for the removal of a

neutron from the i^{th} group, is evidently given by

$$\sigma_a = \sigma_a^c + \sigma_a^i + \sigma_a^e + \sigma_a^f$$

where σ_a^c is the cross section for elastic scattering, σ_a^i

that for inelastic scattering, σ_a^e the cross section for

capture followed by fission, and σ_a^f the cross section for

capture followed by any other reaction, all for neutrons in

the velocity group i . When averaged for isotropic

scattering in the narrow energy range, σ_a^c is given as the

transport cross section.

It is now necessary to examine in detail the source

term $S_0(r)$, in which the fission and capture of neutrons

in velocity group i , apart from those fission or from scattering

from another or the same group, $S_0(r)$ can clearly be

written in the standard form

The present consideration may be roughly stated
included two parts of the discussion on page 20.

$$S_g(r) = \sum_{g'} \sigma_{gg'} N_{g'}(r),$$

where $N_{g'}(r)$ is the total flux in group g' , defined as

$$N_{g'}(r) = \frac{1}{2} \int_{-1}^1 N_{g'}(r, \mu) d\mu.$$

The $\sigma_{gg'}$ (cm^{-1}) are known as transfer coefficients. To determine the form of $\sigma_{gg'}$ from (hopefully) known cross sections, one makes the following definitions:

$\eta_{gg'}$ --- the fraction of neutrons scattered into velocity group g by neutrons of group g' undergoing inelastic (or velocity-degrading) scattering, such that

$$\sum_g \eta_{gg'} = 1,$$

where g and g' are such that $v_g \leq v_{g'}$.

$\nu_{g'}$ --- the average number of neutrons per fission due to a neutron of group g'

$\nu_{gg'}$ --- the relative number of neutrons born into group g per fission due to a neutron of group g' , such that

$$\sum_g \nu_{gg'} = \nu_{g'}.$$

It should be clear that the transfer coefficients are then given by

$$\sigma_{gg'} = \sigma_g^e \delta_g^{g'} + \sigma_g^i \eta_{gg'} + \sigma_g^f \nu_{gg'},$$

where $\delta_g^{g'}$ is the Kronecker delta.

Of the interactions involved above, σ_g^i and σ_g^e may be anisotropic, i.e., may depend on μ . In this case the above equations may still retain approximate validity if σ_g^i and σ_g^e

$$h_{ij}(x) = \frac{W_{ij}}{W} \sigma_{ij}(x)$$

where $h_{ij}(x)$ is the total flux in group i , defined as

$$h_{ij}(x) = \frac{1}{2} \left(h_{ij}(x, y) + h_{ij}(x, -y) \right)$$

The $\sigma_{ij}(x)$ are known as transfer coefficients. To

determine the form of σ_{ij} , from (logically) known cross

sections, one makes the following definitions:

\bar{v}_{ij} -- the fraction of neutrons scattered into

velocity group j by neutrons of group i

undergoing isotropic (or velocity-degrading)

scattering, such that

$$\sum_j \bar{v}_{ij} = 1$$

where i and j are such that $v_j \leq v_i$

\bar{v}_{ij} -- the average number of neutrons per

collision due to a neutron of group i

\bar{v}_{ij} -- the relative number of neutrons born

into group j per collision due to a neutron

of group i , such that

$$\sum_j \bar{v}_{ij} = \bar{v}_{ij}$$

It should be clear that the transfer coefficients are then

given by

$$\sigma_{ij} = \bar{v}_{ij} \sigma_{ij}^c + \bar{v}_{ij} \sigma_{ij}^d + \bar{v}_{ij} \sigma_{ij}^f$$

where σ_{ij}^c is the Knottner delta.

Of the interactions involved above, σ_{ij}^c and σ_{ij}^d may be

anisotropic, i.e., may depend on μ . In this case the above

equations may still retain approximate validity if σ_{ij}^c and σ_{ij}^d

are replaced by corresponding integrals over μ and there is subtracted from $\sigma_{g'}$ and $\sigma_{g'g'}$ a certain parameter correction $\epsilon_{g'}$, defined⁵ as

$$\epsilon_{g'} \equiv \int_{-1}^1 \mu \{ \sigma_{g'}^e(\mu) + \sigma_{g'}^i(\mu) \} d\mu.$$

This transport approximation is apparently accurate, a fact which constitutes its major justification. The alternative to using this approximation is to solve the anisotropic problem.⁶

The transport equation is now completely specified for the case of spherical geometry. One generalization of the equation is possible and, indeed, necessary: a review of the preceding development will reveal that the various cross sections employed may be allowed to depend on the radial coordinate. In particular, it is necessary to let σ be a step function in r , such that σ is zero beyond the radius of the sphere of fissile material.

Preparation of the transport equation for numerical solution by the S_n method is discussed in Carlson's report.⁷ Briefly, the system of differential equations for neutron transport is reduced to a set of coupled difference equations in intervals of r and μ , and these solved by iteration.

⁵Bengt G. Carlson, Solution of the Transport Equation by S_n Approximations (Los Alamos: Los Alamos Scientific Laboratory, 1955), LA-1891, pp. 7-8.

⁶For which see Carlson, ibid., Sec. 9.

⁷Carlson, ibid.

are defined as follows:

$$\epsilon_{\alpha\beta} = \int_{\alpha}^{\beta} \epsilon_{\alpha\beta}^2(x) dx$$

This integral is defined as the difference between the integrals of the squares of the functions ϵ_{α} and ϵ_{β} over the interval $[\alpha, \beta]$.

The response of the system to a step function is given by the integral of the response function over the interval $[\alpha, \beta]$.

For the case of a step function, the response is given by the integral of the response function over the interval $[\alpha, \beta]$.

Preparation of the response function is given by the integral of the response function over the interval $[\alpha, \beta]$.

Explicitly, the response function is given by the integral of the response function over the interval $[\alpha, \beta]$.

The response function is given by the integral of the response function over the interval $[\alpha, \beta]$.

Prepared by the author
in the laboratory of
the author
at the University of
California, Los Angeles

For the present investigation, 8 intervals of μ (the S_8 approximation) and 18 of r were taken, and the problem solved by means of the existing code⁸ for the IBM 704. The cross sections, fission spectrum, etc., used are the six-group set presented in a Los Alamos report⁹ and reproduced in Table 5. The following boundary conditions are necessary to complete the specification of the problem for the bare sphere:

- a) Conservation of flux at the center:

$$N(0, \mu) = N(0, -\mu)$$

- b) Derivation of all neutrons from the critical assembly:

$$N(a, -\mu) = 0,$$

where a is the radius of the assembly.

Among the output of the computer is the relative neutron leakage flux in each energy interval used. For comparison with the experimentally determined spectrum, the theoretical leakage spectrum is normalized so that

$$\sum_{g=3}^6 N_g = 1,$$

⁸Bengt G. Carlson, The S_n Method and the SNG Code (Los Alamos: Los Alamos Scientific Laboratory, 1959), LAMS-2201.

⁹Gordon E. Hansen and William H. Roach, Six and Sixteen Group Cross Sections for Fast and Intermediate Critical Assemblies (Los Alamos: Los Alamos Scientific Laboratory, 1961), LAMS-2543. These cross sections must be multiplied by the number of nuclei per cm^3 . Since Jezebel U233 contained some U234 (1.24%) and U238 (0.06%), the cross sections for U233 were corrected slightly by taking a weighted average. The stated composition corresponds to a density of 18.45 gm/cm^3 .

For the present investigation, 8 intervals of Δ (the Δ approximated) and 15 of τ were taken, and the problem solved by means of the rotating code⁶ for the IBM 704. The cross sections, fission spectrum, etc., used are the six-group set presented in a Los Alamos report⁷ and reproduced in Table 2. The following boundary conditions are necessary to complete the specification of the problem for the bare spheres:

- a) Conservation of flux at the center:

$$K(0, \mu) = K(0, -\mu)$$
- b) Derivation of all neutrons from the original assembly:

$$K(a, -\mu) = 0,$$

where a is the radius of the assembly.

Among the output of the computer is the relative neutron leakage flux in each energy interval used. For comparison with the experimentally determined spectrum, the theoretical leakage spectrum is normalized so that

$$\frac{M}{M_0} = 1,$$

⁶Henry G. Carlson, The Δ Method and the IBM Code (Los Alamos Scientific Laboratory, 1959), LAMS-2201.

⁷Gordon E. Hansen and William H. Rosen, Six and Sixteen Group Cross Sections for Fast and Intermediate Critical Assemblies (Los Alamos Scientific Laboratory, 1961), LAMS-22-5. These cross sections were multiplied by the number of nuclei per cm³. Since Lamos 2233 contained some U235 (1.7%) and U238 (0.03%), the cross sections for U235 were corrected slightly by taking a weighted average. The stated composition corresponds to a density of 18.5 gm/cm³.

TABLE 5
 SIX GROUP PARAMETERS FOR U²³³
 (CROSS SECTIONS IN BARNS)

| Group No. | 1 | 2 | 3 | 4 | 5 | 6 |
|------------------------------|-------|---------|---------|---------|---------|-------|
| Energy Range, Mev | 0-0.1 | 0.1-0.4 | 0.4-0.9 | 0.9-1.4 | 1.4-3.0 | 3.0-∞ |
| Fission Spectrum | 0.014 | 0.090 | 0.180 | 0.168 | 0.344 | 0.204 |
| ν_g | 2.51 | 2.53 | 2.57 | 2.61 | 2.70 | 3.02 |
| σ_f | 3.23 | 2.24 | 1.94 | 1.89 | 1.83 | 1.75 |
| σ_a | 0.40 | 0.15 | 0.11 | 0.08 | 0.06 | 0.04 |
| $\sigma_{\text{transport}}$ | 11.8 | 8.1 | 5.3 | 4.6 | 4.5 | 4.25 |
| $\sigma_{g \rightarrow g}$ | 8.17 | 5.66 | 2.91 | 1.82 | 1.53 | 1.19 |
| $\sigma_{g \rightarrow g-1}$ | | 0.05 | 0.29 | 0.45 | 0.18 | 0.20 |
| $\sigma_{g \rightarrow g-2}$ | | | 0.05 | 0.30 | 0.50 | 0.27 |
| $\sigma_{g \rightarrow g-3}$ | | | | 0.06 | 0.35 | 0.45 |
| $\sigma_{g \rightarrow g-4}$ | | | | | 0.05 | 0.31 |
| $\sigma_{g \rightarrow g-5}$ | | | | | | 0.04 |
| $\nu_g \sigma_f$ | 8.107 | 5.667 | 4.986 | 4.933 | 4.941 | 5.285 |

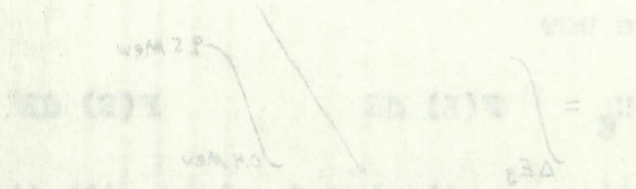
and then N_g , the neutron flux in energy group g , is divided by E_g , the width of the g^{th} group in Mev. (For group 6, E_g is taken as 6.5 Mev; i.e., it is assumed that there are no neutrons with energies greater than 9.5 Mev.) This normalization yields neutrons $\text{cm}^{-2}/\text{Mev}$. The experimental spectrum is lumped into the same four groups in a similar manner, where now

$$N_g = \frac{\int_{\Delta E_g} F(E) dE}{\int_{0.4 \text{ Mev}}^{9.5 \text{ Mev}} F(E) dE}$$

These quantities are displayed, along with the ratio of the theoretically calculated and experimentally measured quantities, in Table 6. Included in this table are the same quantities for the bare-sphere assemblies Jezebel Pu^{239} and Godiva U^{235} .¹⁰ It is seen that the theoretical result is not in violent disagreement with that observed; certainly, no condemnation of the cross sections, etc., employed in the theoretical treatment can be made on this basis.

¹⁰L. Stewart, Leakage Neutron Spectrum.

and then ν_{max} is divided by ν_{min} the ratio of the ν_{max} group is found. (For groups ν_{max} is taken as 0.5 ν_{min} ; it is assumed that there are no overtones with energies greater than 0.5 ν_{min}). This normalized yields numbers of ν_{max} . The experimental spectrum is lumped into the same four groups in a similar manner, where ν_{max}



These quantities are displayed, along with the ratio of the theoretically calculated and experimentally measured quantities, in Table 6. Included in this table are the same quantities for the two-photon absorption lines labeled ν_{max} and ν_{min} . It is seen that the theoretical results are not in violent disagreement with those observed, certainly, no consideration of the cross sections, etc., employed in the theoretical treatment can be made on this basis.

101. Stewart, Richard Lewis, *Phys. Rev.*

TABLE 6
COMPARISON OF THEORETICAL AND EXPERIMENTAL LEAKAGE SPECTRA

| | 0.4-0.9 Mev | 0.9-1.4 Mev | 1.4-3.0 Mev | 3.0-∞ Mev |
|---------------------------|----------------|----------------|----------------|--------------|
| Jezebel Pu ²³⁹ | | | | |
| Theoretical | 0.481 | 0.390 | 0.216 | 0.034 |
| Experimental | 0.488 | 0.342 | 0.211 | 0.038 |
| Ratio ^a | 0.99 | 1.14 | 1.02 | 0.89 |
| Jezebel U ²³³ | | | | |
| Theoretical | 0.513 | 0.384 | 0.218 | 0.031 |
| Experimental | 0.510 | 0.372 | 0.203 | 0.036 |
| Ratio ^a | 1.01 | 1.03 | 1.07 | 0.86 |
| Godiva U ²³⁵ | | | | |
| Theoretical | 0.634 | 0.392 | 0.197 | 0.026 |
| Experimental | 0.658 | 0.392 | 0.189 | 0.027 |
| Ratio ^a | 0.96 | 1.00 | 1.04 | 0.96 |

^aTheoretical flux/Experimental flux.

COMPARISON OF THEORETICAL AND EXPERIMENTAL RESULTS

| Case No. | Theoretical Value | Experimental Value | Ratio | Remarks |
|----------|-------------------|--------------------|-------|--------------|
| 1 | 0.15 | 0.14 | 0.93 | Theoretical |
| 2 | 0.25 | 0.24 | 0.96 | Experimental |
| 3 | 0.35 | 0.34 | 0.97 | Ratio |
| 4 | 0.45 | 0.44 | 0.98 | Theoretical |
| 5 | 0.55 | 0.54 | 0.98 | Experimental |
| 6 | 0.65 | 0.64 | 0.98 | Ratio |
| 7 | 0.75 | 0.74 | 0.99 | Theoretical |
| 8 | 0.85 | 0.84 | 0.99 | Experimental |
| 9 | 0.95 | 0.94 | 0.99 | Ratio |

Journal of the Institution of Engineers

APPENDIX A
CALCULATION OF Ω

Elementary considerations of collisions between equally massive particles yield the results

$$d^2\Omega_{\text{LAB}} \equiv d^2\Theta = \sin\theta \, d\theta \, d\phi,$$

$$d^2\Omega_{\text{CM}} \equiv d^2\Omega = 4 \cos\theta \, d^2\Theta = 4 \cos\theta \sin\theta \, d\theta \, d\phi,$$

where all angles are measured in the laboratory reference frame. Along the edge AB (Fig. 8) one has

$$z = \rho \cos\theta = \text{const.},$$

$$x = \rho \sin\theta \cos\phi = \text{const.},$$

whence

$$\frac{x}{z} = \tan\theta \cos\phi = \tan\alpha,$$

where α is the maximum permissible value of the horizontal or dip angle (assumed equal in this analysis); i.e., α is the half angle of the pyramid of acceptance. Thus

$$\theta = \tan^{-1} \left(\frac{\tan\alpha}{\cos\phi} \right)$$

along edge AB. It follows that

$$\begin{aligned} \Omega &= 8 \int_0^{\pi/4} \int_0^{\tan^{-1}(\frac{\tan\alpha}{\cos\phi})} 4 \cos\theta \sin\theta \, d\theta \, d\phi \\ &= 32 \int_0^{\pi/4} \int_0^{\cos^{-1}(\frac{\cos\phi}{\sqrt{\cos^2\phi + \tan^2\alpha})} \cos\theta \sin\theta \, d\theta \, d\phi \\ &= 16 \tan^2\alpha \int_0^{\pi/4} \frac{d\phi}{\tan^2\alpha + \cos^2\phi}. \end{aligned}$$

The angle θ is defined as the angle between the normal to the surface and the direction of the incident ray.

$$\frac{\sin \theta_i}{v_i} = \frac{\sin \theta_r}{v_r}$$

where θ_i is the angle of incidence, θ_r is the angle of reflection, v_i is the speed of light in the incident medium, and v_r is the speed of light in the reflecting medium.

$$\frac{\sin \theta_i}{v_i} = \frac{\sin \theta_r}{v_r}$$

where θ_i is the angle of incidence, θ_r is the angle of reflection, v_i is the speed of light in the incident medium, and v_r is the speed of light in the reflecting medium.

where α is the angle between the normal to the surface and the direction of the incident ray.

or the angle between the normal to the surface and the direction of the incident ray.

the half angle of the ray is θ .

$$\theta = \frac{\alpha}{2}$$

$$\frac{\sin \theta_i}{v_i} = \frac{\sin \theta_r}{v_r}$$

$$\frac{\sin \theta_i}{v_i} = \frac{\sin \theta_r}{v_r}$$

$$\frac{\sin \theta_i}{v_i} = \frac{\sin \theta_r}{v_r}$$

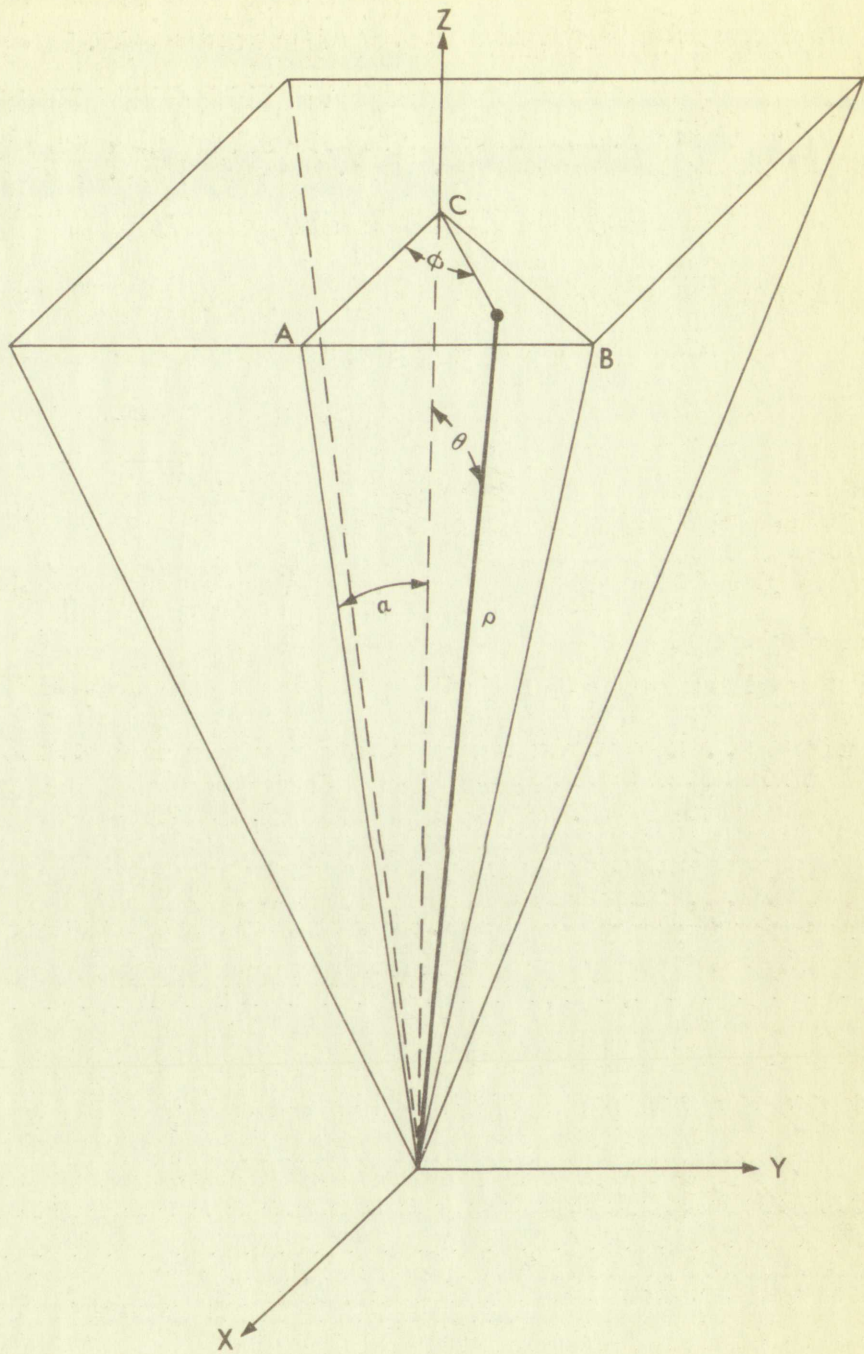
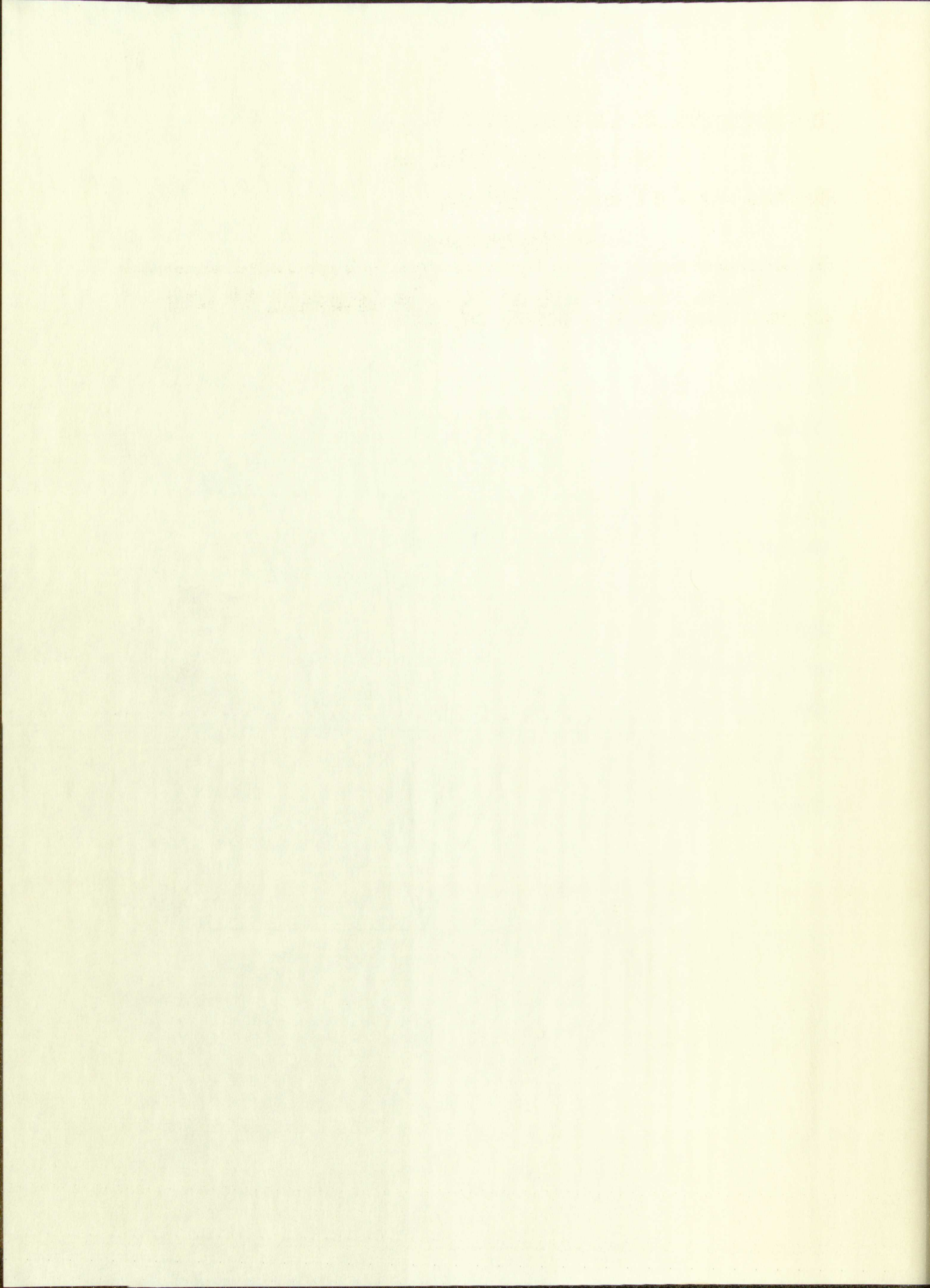


Fig. 8.



Evaluating the final integral,¹

$$\Omega = 16 \sin \alpha \tan^{-1}(\sin \alpha).$$

For the case at hand $\alpha = 16^\circ$ and

$$\Omega = 1.186 \text{ steradians.}$$

¹B. O. Pierce, A Short Table of Integrals (3^d ed.; Boston: Ginn and Co., 1929), No. 315.

Inventory of the ...

U.S. ...

For the year ...

U.S. ...

In ...
Boston: ...

MASSACHUSETTS

STATE

INDUSTRY

AND

COMMERCE

19...

APPENDIX B

APPROXIMATE CALCULATION OF $\overline{\cos^2 \psi}$

To sufficient accuracy (1%) the square-based pyramidal solid angle of observation may be considered replaced by a right circular cone such that both bases have the same area. Let a be the length of the edge of the pyramid and b the slant height of the cone. Then, if α be the half-angle for the pyramid and ψ_{\max} that of the cone,

$$\pi a^2 \sin^2 \psi_{\max} = 4 b^2 \sin^2 \alpha,$$

whence, to a good approximation for α and ψ_{\max} small,

$$\pi \sin^2 \psi_{\max} = 4 \sin^2 \alpha.$$

Thus, since in the laboratory system $\frac{d\sigma}{d\Omega} = 4\sigma \cos \theta$,

$$\begin{aligned} \overline{\cos^2 \psi} &= \frac{\int_0^{\psi_{\max}} \cos^2 \psi \cdot 2\pi \sin \psi \cdot 4\sigma \cos \psi \, d\psi}{\int_0^{\psi_{\max}} 2\pi \sin \psi \cdot 4\sigma \cos \psi \, d\psi} \\ &= \frac{1}{2} (\cos^2 \psi_{\max} + 1). \end{aligned}$$

For $\alpha = 16^\circ$, $\psi_{\max} = 18^\circ 7'$, and $\overline{\cos^2 \psi} = 0.952$.

APPENDIX B

ANALYTICAL CALCULATION OF ψ

In addition to the above, the following conditions must be satisfied by a valid set of observations: the observations must be consistent with the right-angle condition and must not have been taken from the same station. Let α be the length of the side of the pyramid and h the height of the cone. Then, $L \propto h$ for the half-angle.

for the pyramid and ψ the half of the cone,

$$\pi \sin^2 \alpha = \psi \sin^2 \alpha$$

whence, to a good approximation for α and ψ small,

$$\pi \sin^2 \alpha = \psi \sin^2 \alpha$$

Thus, also in the laboratory space, $\Theta \cos \psi = \frac{h}{L} \cos \psi$

$$\psi = \frac{\int_0^{\psi} \sin^2 \alpha \, d\alpha}{\int_0^{\psi} \sin^2 \alpha \, d\alpha} = \frac{\psi \cos \psi}{\psi \cos \psi}$$

$$\psi \cos \psi = \psi \cos \psi$$

$$\psi \cos \psi = \psi \cos \psi$$

$$\text{For } \alpha = 10^\circ, \psi = 10^\circ, \text{ and } \cos \psi = 0.985$$

APPENDIX C

RAW DATA

| E_n (MeV) | N_p | Volume Scanned (cm^3) | E_n (MeV) | N_p | Volume Scanned (cm^3) |
|----------------|-------|--|----------------|-------|--|
| 0.35 | 86 | 0.475×10^{-4} | 4.35 | 12 | 5.740×10^{-4} |
| 0.45 | 54 | " | 4.45 | 12 | " |
| 0.55 | 47 | " | 4.55 | 19 | " |
| 0.65 | 142 | 1.924×10^{-4} | 4.65 | 11 | " |
| 0.75 | 122 | " | 4.75 | 7 | " |
| 0.85 | 98 | " | 4.85 | 9 | " |
| 0.95 | 70 | " | 4.95 | 10 | " |
| 1.05 | 89 | " | 5.05 | 17 | " |
| 1.15 | 82 | " | 5.15 | 12 | " |
| 1.25 | 98 | " | 5.25 | 10 | " |
| 1.35 | 48 | " | 5.35 | 8 | " |
| 1.45 | 57 | " | 5.45 | 7 | " |
| 1.55 | 51 | " | 5.55 | 7 | " |
| 1.65 | 40 | " | 5.65 | 9 | " |
| 1.75 | 45 | " | 5.75 | 9 | " |
| 1.85 | 35 | " | 5.85 | 2 | " |
| 1.95 | 69 | 3.834×10^{-4} | 5.95 | 4 | " |
| 2.05 | 50 | " | 6.05 | 2 | " |
| 2.15 | 63 | " | 6.15 | 4 | " |
| 2.25 | 60 | " | 6.25 | 3 | " |
| 2.35 | 48 | " | 6.35 | 4 | " |
| 2.45 | 46 | 4.315×10^{-4} | 6.45 | 1 | " |
| 2.55 | 66 | 4.800×10^{-4} | 6.55 | 4 | " |
| 2.65 | 59 | " | 6.65 | 4 | " |
| 2.75 | 43 | " | 6.75 | 2 | " |
| 2.85 | 46 | " | 6.85 | | " |
| 2.95 | 42 | " | 6.95 | 3 | " |
| 3.05 | 37 | " | 7.05 | | " |
| 3.15 | 37 | " | 7.15 | 1 | " |
| 3.25 | 33 | " | 7.25 | 1 | " |
| 3.35 | 33 | " | 7.35 | 2 | " |
| 3.45 | 34 | 5.740×10^{-4} | 7.45 | 1 | " |
| 3.55 | 29 | " | 7.55 | 2 | " |
| 3.65 | 32 | " | 7.65 | 2 | " |
| 3.75 | 20 | " | 7.75 | 1 | " |
| 3.85 | 34 | " | 8.25 | 1 | " |
| 3.95 | 36 | " | 8.65 | 3 | " |
| 4.05 | 23 | " | 9.05 | 1 | " |
| 4.15 | 20 | " | 9.25 | 1 | " |
| 4.25 | 16 | " | 9.35 | 1 | " |



STATE OF TEXAS
COMMISSIONERS OF THE GENERAL LAND OFFICE

| Section | Block | Acres | Original Grantee | Acres | Value (1901) |
|---------|-------|-------|------------------|-------|--------------|
| 1 | 1 | 10.00 | ... | 10.00 | 0.32 |
| 1 | 2 | 10.00 | ... | 10.00 | 0.42 |
| 1 | 3 | 10.00 | ... | 10.00 | 0.52 |
| 1 | 4 | 10.00 | ... | 10.00 | 0.62 |
| 1 | 5 | 10.00 | ... | 10.00 | 0.72 |
| 1 | 6 | 10.00 | ... | 10.00 | 0.82 |
| 1 | 7 | 10.00 | ... | 10.00 | 0.92 |
| 1 | 8 | 10.00 | ... | 10.00 | 1.02 |
| 1 | 9 | 10.00 | ... | 10.00 | 1.12 |
| 1 | 10 | 10.00 | ... | 10.00 | 1.22 |
| 1 | 11 | 10.00 | ... | 10.00 | 1.32 |
| 1 | 12 | 10.00 | ... | 10.00 | 1.42 |
| 1 | 13 | 10.00 | ... | 10.00 | 1.52 |
| 1 | 14 | 10.00 | ... | 10.00 | 1.62 |
| 1 | 15 | 10.00 | ... | 10.00 | 1.72 |
| 1 | 16 | 10.00 | ... | 10.00 | 1.82 |
| 1 | 17 | 10.00 | ... | 10.00 | 1.92 |
| 1 | 18 | 10.00 | ... | 10.00 | 2.02 |
| 1 | 19 | 10.00 | ... | 10.00 | 2.12 |
| 1 | 20 | 10.00 | ... | 10.00 | 2.22 |
| 1 | 21 | 10.00 | ... | 10.00 | 2.32 |
| 1 | 22 | 10.00 | ... | 10.00 | 2.42 |
| 1 | 23 | 10.00 | ... | 10.00 | 2.52 |
| 1 | 24 | 10.00 | ... | 10.00 | 2.62 |
| 1 | 25 | 10.00 | ... | 10.00 | 2.72 |
| 1 | 26 | 10.00 | ... | 10.00 | 2.82 |
| 1 | 27 | 10.00 | ... | 10.00 | 2.92 |
| 1 | 28 | 10.00 | ... | 10.00 | 3.02 |
| 1 | 29 | 10.00 | ... | 10.00 | 3.12 |
| 1 | 30 | 10.00 | ... | 10.00 | 3.22 |
| 1 | 31 | 10.00 | ... | 10.00 | 3.32 |
| 1 | 32 | 10.00 | ... | 10.00 | 3.42 |
| 1 | 33 | 10.00 | ... | 10.00 | 3.52 |
| 1 | 34 | 10.00 | ... | 10.00 | 3.62 |
| 1 | 35 | 10.00 | ... | 10.00 | 3.72 |
| 1 | 36 | 10.00 | ... | 10.00 | 3.82 |
| 1 | 37 | 10.00 | ... | 10.00 | 3.92 |
| 1 | 38 | 10.00 | ... | 10.00 | 4.02 |
| 1 | 39 | 10.00 | ... | 10.00 | 4.12 |
| 1 | 40 | 10.00 | ... | 10.00 | 4.22 |



COMMISSIONERS OF THE GENERAL LAND OFFICE
STATE OF TEXAS
GENERAL LAND OFFICE
DAVIDSON

W
TAYLOR'S
ALUMINUM
WHITE
BOARD
CO.

ALUMINUM UNIT

1912
MAY 10 1912
RECEIVED
LIBRARY
OF THE
MUSEUM OF NATURAL HISTORY
AND
ETHNOLOGY
OF THE
SMITHSONIAN INSTITUTION
WASHINGTON, D. C.



